JAERI-Tech
2004-079

CALCULATION OF AGE-DEPENDENT DOSE CONVERSION COEFFICIENTS FOR RADIONUCLIDES UNIFORMLY DISTRIBUTED IN AIR

February 2005

Tran Van HUNG , Daiki SATOH, Fumiaki TAKAHASHI, Shuichi TSUDA,
Akira ENDO, Kimiaki SAITO and Yasuhiro YAMAGUCHI

日本原子力研究所
Japan Atomic Energy Research Institute

本レポートは，日本原子力研究所が不定期に公刊している研究報告書です。
入手の問合わせは，日本原子力研究所研究情報部研究情報課（〒319-1195　茨城県那珂郡東海村）あて，お申し越しください。なお，このほかに財団法人原子力弘済会資料センター（〒319-1195　茨城県那珂郡東海村日本原子力研究所内）で複写による実費頒布をおこなっております。

This report is issued irregularly.
Inquiries about availability of the reports should be addressed to Research Information Division, Department of Intellectual Resources, Japan Atomic Energy Research Institute, Tokai-mura, Naka-gun, Ibaraki-ken, 319-1195, Japan.

編集兼発行　　日本原子力研究所

JAERI-Tech 2004-079

Calculation of Age-dependent Dose Conversion Coefficients for Radionuclides Uniformly Distributed in Air

Tran Van HUNG※, Daiki SATOH, Fumiaki TAKAHASHI, Shuichi TSUDA, Akira ENDO, Kimiaki SAITO and Yasuhiro YAMAGUCHI

Department of Health Physics
Tokai Research Establishment
Japan Atomic Energy Research Institute
Tokai-mura, Naka-gun, Ibaraki-ken

(Received December 8, 2004)

Age-dependent dose conversion coefficients for external exposure to photons emitted by radionuclides uniformly distributed in air were calculated. The size of the source region in the calculation was assumed to be effectively semi-infinite in extent. Firstly, organ doses were calculated with a series of age-specific MIRD-5 type phantoms using MCNP code, a Monte Carlo transport code. The calculations were performed for mono-energetic photon sources of twelve energies from 10 keV to 5 MeV and for phantoms of newborn, 1, 5, 10 and 15 years, and adult. Then, the effective doses to the different age-phantoms from the mono-energetic photon sources were estimated based on the obtained organ doses. The calculated effective doses were used to interpolate the conversion coefficients of the effective doses for 160 radionuclides, which are important for dose assessment of nuclear facilities. In the calculation, energies and intensities of emitted photons from radionuclides were taken from DECDC, a recent compilation of decay data for radiation dosimetry developed at JAERI. The results are tabulated in the form of effective dose per unit concettration and time (Sv per Bq s m^{-3}).

Keywords: Organ Dose, Effective Dose, Conversion Coefficient, Age-dependent Coefficient, MIRD-5 Type Phantom, MCNP Code, Semi-infinite Source, Radionuclides, Air Submersion, DECDC

※ MEXT Nuclear Researchers Exchange Program (Research and Development Center for Radiation Technology, Vietnam Atomic Energy Commission, VIETNAM)

JAERI-Tech　2004-079

空気中に一様分布する放射性核種に対する年齢依存線量換算係数の計算

日本原子力研究所東海研究所保健物理部
Tran Van HUNG※・佐藤　大樹・高橋　史明・津田　修一・
遠藤　章・斎藤　公明・山口　恭弘

（2004年12月8日受理）

空気中に一様分布する光子放出核種による外部被ばくに対し，年齢依存線量換算係数を計算した。一連の年齢別数学ファントム及びモンテカルロ放射線輸送コード MCNP を用いて，半無限の空気中線源からの照射による臓器及び組織線量を計算した。臓器線量は，10 keV から 5 MeV までの 12 種類の単一エネルギー線源について，新生児，1，5，10，15 歳及び成人の 6 年齢群に対して計算した。得られた臓器線量に基づき，各光子エネルギー及び年齢群に対する実効線量を算定した。そして，実効線量のエネルギー依存性を内挿し，原子力施設の安全評価上重要とされる 160 核種に対する実効線量換算係数を計算した。各放射性核種からの放出光子エネルギー及び放出率は，原研で開発された線量計算用崩壊データ DECDC のデータを用いた。換算係数は，単位濃度及び時間あたりの実効線量(Sv per Bq s m^{-3})で与えた。

東海研究所：〒319-1195　茨城県那珂郡東海村白方白根 2-4
※文部科学省原子力研究交流制度研究員（ベトナム原子力委員会放射線技術研究開発センター）

Contents

目　次

This is a blank page.

1. Introduction

Since the year 1990, the International Commission on Radiological Protection (ICRP) has recommended effective dose, E, as an index of individual exposure. It is related to stochastic effect on the human body when several organs receive different doses from radiation. This recommendation was conformed to the International Basic Safety Standards. However, this quantity cannot be measured or assessed directly. ICRP[1)] and the International Commission on Radiation Units and Measurements (ICRU)[2)] recommended the use of operational dosimetric quantities as a surrogate of E for the monitoring of individual exposure. It is necessary to determine conversion coefficients from a measurable quantity (i.e. activity of the source, air kerma, etc.) to the un-measurable quantities of organ doses. For this purpose, Monte Carlo techniques in conjunction with anthropomorphic mathematical models are useful. Monte Carlo techniques can deal with complex irradiation conditions and provide absorbed dose distributions in human body in a variety of exposure situations. The effective dose E, or the predecessor, the effective dose equivalent H_E, is the sum of organ and tissue equivalent dose multiplied by appropriate weighting factors.

The conversion coefficients of organ dose, effective dose equivalent and effective dose have been studied more than three decades for external exposure to photon emitters from different contaminated environments, such as soil, air and water. Various studies[3-15)] have been made in this field. A number of dose coefficients were calculated for external exposure of the body from photon sources distributed in the environment. However, the data were mainly for adult. Saito and Jacob[7)] performed one of the most complete studies for natural sources uniformly distributed using a Monte Carlo method. Eckerman and Ryman[8)] adopted a combination of discrete ordinates and Monte Carlo methods to solve photon transport equation for photon emitters distributed in the environment, in which the calculation was divided into two steps: (1) the calculation of the radiation field incident on the cylindrical suface surrounding the human model, and (2) the calculation of organ dose due to a surface source equivalent to the angular flow rate entering the cylinder surrounding the phantom. The advantage of their method is to avoid difficulties due to the combination of deep penetration (i.e., transport through many mean free paths of air and/or soil) and the complex geometry (the human phantom) and to overcome other limitations of earlier calculation.

Radiation dose depends strongly on the temporal and spatial distribution of the radionuclides to which a human is exposed. The estimation of the dose to the body from radiation emitted by an arbitrary distribution of a radionuclide in an environmental medium is extremely difficult. Therefore, the calculation is performed with simplified and idealized exposure geometries; i.e., the size of radiation source is effectively infinite or semi-infinite and the concentration of radionuclide is uniform in the source region. In addition, various variance reduction techniques are necessary to improve calculation efficiency.

The present work aimed to obtain the age-dependent dose conversion coefficients for radionuclides uniformly distributed in a semi-infinite cloud. The energy and angular distributions of photon field, organ dose and effective dose for external exposure from the mono-energetic photon sources were calculated using the MCNP code.[16)] The studies were performed with age-specific phantoms based on the MIRD-5 phantoms: newborn, 1, 5, 10 and 15 years, and adult. In the calculation, some variance reduction techniques in the MCNP code were used.

2. Calculation

2.1 Radiation Transport Code and Cross-section Data

The MCNP code version 4B[16] was used for the calculation of the photon transport in this work. MCNP is a general-purpose code, which was developed at the Los Alamos National Laboratory, and can be used for radiation transport in complicated three-dimensional configurations. It can treat neutron, photon and electron transport. For photons, the code takes account of incoherent and coherent scattering, the possibility of fluorescent emission after photoelectric absorption, absorption in pair production with local emission of annihilation radiation and bremsstrahlung.

The photon cross sections used in this work were based on the evaluated data from ENDF[17] from 1 keV to 100 MeV. The fluorescence data were taken from work by Everett and Cashwell's work.[18]

2.2 Mathematical Phantom

For the organ dose calculations, six MIRD-5 type phantoms that represent newborn, 1, 5, 10 and 15 years old and adult were employed. These phantoms designed by Eckerman *et al.*[19] are representative models of large western populations and are widely used in calculations of organ doses. The descriptions of the interior organs, while approximately correct as to size, shape, position, composition and density, are simplified to provide formulas which are readily evaluated by a digital computer. All the phantoms are hermaphroditic.

The phantoms consist of three tissue types: skeletal, lung, and soft tissues. The elemental compositions of the tissues are given in Table 1 along with their densities. The elemental composition and density of newborn are different from those of adult in water content and bone mineral content. The data of the elemental compositions were taken from ORNL's data,[20] which slightly differ from those given by Snyder *et al.*[21] Compared the densities with those assigned by Snyder *et al.*, the densities used in this work (except newborn) were changed from 1.4862 to 1.4 g cm^{-3} for skeletal tissue and from 0.9869 to 1.04 g cm^{-3} for soft tissue. The lung density was unchanged but was rounded to three significant digits.

2.3 Geometry and Compositions of Source

Since the size of the source region can be several hundred meters, it is important to carry out the calculation effectively. One of most important subjects in this study is to determine appropriate radius of the source region in air and thickness in soil. The geometry of the present calculation using the MCNP code is shown in Fig. 1. It includes source regions of air and soil. The source region of air is represented using a hemisphere with radius of R. The photons are mono-energetic and the radionuclide in the source region is uniformly distributed with unit strength (1 Bq m^{-3}). In the calculation of organ dose, the MIRD-5 type phantoms with various ages are set on the ground and surrounding by a semi-infinite cloud source with the minimum radius R_{min}.

The soil region is represented by a disk with a radius of R and a thickness of d . In all the calculations, the thickness of soil was set to be six mean free paths (mfp) of the source energy. These thicknesses of soil ensure that photon scattered beyond the boundary between air and soil would travel a minimum of twelve mean free paths to reach the phantom location, and then there is no significant contribution to organ doses.

The soil and air compositions are given in Table 2.[8] For the air, this composition is under the conditions of 40 % relative humidity, a pressure of 1.013×10^5 Pa, a temperature of 293 K, and a density of 1.2×10^{-6} kg m^{-3}. For the soil, this composition is the typical silty soil containing 30% water and 20 % air by volume. The soil density was taken to be 1.6×10^{-3} kg m^{-3}.

2.4 Procedures

2.4.1 Determination of minimum radius of source region

To calculate the organ doses in the phantoms effectively, it is important to optimize the size of the source region, since the organ doses depend on the size of radiation source. The minimum radius of source region, R_{min}, can be assumed to be effectively semi-infinite in extent, if it can contribute at least 99 % to the exposure from a semi-infinite source. The radius of the source region, R, was determinated in terms of the mean free path of photons at initial energy. The mean free path of photons is defined as the inverse of the linear attenuation coefficient μ' of the medium through which the radiations are transported. The coefficient is the sum of the coefficients from photoelectric absorption, Compton scattering, and pair production. The mass attenuation coefficient μ'/ρ for the air and the soil are shown in Table 3.

The kerma in the air, K_{air}, at 1 m above the ground with different source radius R were calculated in the geometry shown in Fig. 1. K_{air} depends on the source radius and is a function of radius R. The minimum radius R_{min} can be deteminated, when $K_{air}(R)$ becomes constant.

The kerma $K_{air}(R)$ in the air at 1 m above the ground for a photon emitter of energy E_0, uniformly distributed in air were calculated by:

$$K_{air}(R) = \sum_i k(E_i)\Phi_i(E_i, R) \qquad (1)$$

where E_i is the average energy in energy bin, $\Phi_i(E_i, R)$ is the photon fluence per unit activity per m^3 of air in energy bin for the source radius of R, and $k(E_i)$ is conversion coefficient for air kerma per unit fluence of monoenergetic photons. The conversion coefficients $k(E_i)$ were taken from ICRP publication 74.[22] The photon fluence $\Phi_i(E_i, R)$ was calculated using a point detector, located at 1 m above the ground, of the MCNP code (tally F5). The point detector tally can provide a good estimate of the particle flux in a point.

Several variance reduction techniques were adopted for efficient simulation of particle transport. To improve the source sampling, a DXTRAN sphere of 50 cm radius surrounded by the point detector was used. The DXTRAN is a variance reduction technique used in the MCNP code. The DXTRAN technique is typically used when a small region is being inadequately sampled because particles have a very small probability of scattering toward that region. Source biasing with the SB card of MCNP was also used to increase the sampling in importance region and to improve the convergence rate of the problem.

2.4.2 Photon spectral distribution

The organ doses are dependent on energy and incident direction of photons. It is important to understand the characteristics of radiation field, where the phantom is placed. Then, energy distribution of the photon fluence, $\Phi(E)$, and its angular distribution, $\Phi(E, \theta)$, at the height of 1 m above the ground were calculated. The photon sources were homogeneous semi-infinite clouds with the minimum radius discussed above. The energy distribution of the

photon fluence $\Phi(E)$ at 1 m above the ground were calculated using a point detector and an average fluence tally across a surface surrounding the calculation point (F2 tally). The F2 tally is a surface tally in the MCNP code. In the calculation of average fluence across a surface, a spherical surface with radius of 50 cm was used and located at 1 m above the ground.

The angular distribution, $\Phi(E, \theta)$, which is called double differential energy fluence, is the average fluence across a spherical surface to different incident angle of photon. A spherical surface with radius of 50 cm was used and located at 1 m above the ground. Since the source distribution is homogeneous and the calculation geometry is symmetric to z-direction, the photon spectral distribution around the azimuth angle is uniform from 0° to 360°. The photon spectral distribution was calculated to polar angle. To improve the source sampling, as well as in the estimation of the minimum radius of source region, R_{min}, the DXTRAN sphere with radius of 52 cm was used.

2.4.3 Organ doses from mono-energetic source

The calculation of organ doses from exposure of the human body to photon emitters distributed in the environment requires the solution of a complex radiation transport problem. To obtain organ doses from various kinds of radionuclides, it is efficient to use a data table of organ doses as a function of photon energy. In this work, equivalent dose in organ, H_T, and effective dose, E, for mono-energetic photon sources at twelve energies from 0.01 to 5 MeV were calculated using the six MIRD-5 phantoms of different ages.

The organ equivalent doses and effective doses were calculated for whole body exposure with a monoenegetic photon source, uniformly distributed in air. All phantoms used in the calculation (including newborn phantom) were modeled to stand vertically on the ground at air-ground interface, although for the newborn and 1-year old, this is an unrealistic position; this assumption was made in order to assess the effect of body size on the dose and to be able to interpolate for intermediate sizes.

The organ doses were calculated using the F6 tally based on track length estimation in the MCNP code. The F6 tally can calculate the heating and energy deposition in the certain region. However, F6 tally is normalized to be per source particle and unit of F6 is MeV g^{-1}. To obtain the energy deposited in the organ or tissues in terms of gray unit, Gy, we have to normalize using the following conversion factor:

$$f_m = \left[\frac{1.602x10^{-6}\, ergs/MeV}{100 ergs/g} \times 100^{-1}\right] \times \left[\frac{2}{3}\pi(R_{\min})^3 \eta\right] \qquad (2)$$

where the first square bracket is a factor that converts the unit from MeV g^{-1} to Gy, and the second square bracket is a factor in terms of strength of radiation source. The strength is equal to the volume of source region (m^3) multiplied by the radioactive concentration in the air η (Bq m^{-3}). The organ doses in Gy unit were calculated by using F6 tally in conjunction with f_m factor on the companion card FM6.

For the calculation of doses of cortical bone and red bone marrow, the kerma approximation was applied. The kerma factors for photon in a specified tissue (or organ) were calculated by summing the products of the mass fraction of element in tissue, the photon energy, and the mass energy-transfer coefficient of the element for photons of that energy. The kerma factors for photon in cortical bone and red bone marrow were obtained from reference,[23] based on the energy transfer coefficients of Hubbell.[24]

The effective dose E was calculated by following formula:

$$E = \sum_T w_T H_T \tag{3}$$

where w_T is the tissue weighting factor of organ T. The values of w_T recommended in ICRP Publication 60[1] were applied to all the age groups considered.

2.4.4 Conversion coefficients of effective dose for radionuclides

Due to smooth dose-energy dependence, a set of the effective doses for monoenergetic sources allows one to interpolate effective doses for other energies. The interpolation was carried out with a 4-point (cubic) Lagrangian interpolation formula at twelve energies from 10 keV to 5 MeV. The conversion coefficients of the effective dose for radionuclides can be then calculated by the following equation:

$$g^N = \sum_i y_i^N F(E_i) \tag{4}$$

where y_i^N (in $\gamma.s^{-1}.Bq^{-1}$) is the yield of photons with energy E_i per disintergration, $F(E_i)$ is the interpolation functions and the sum is taken over the photon energies of emission spectrum of radionuclide N.

In this work, the conversion coefficients of the effective doses for 160 radionuclides, which are important for safety assessment of nuclear facilities, were calculated. The nuclear data of these radionuclides were taken from DECDC.[25] The DECDC was developed at JAERI and addresses 1027 radionuclides, including all the nuclides of ICRP Publication 38.

3. Results and Discussion

3.1 Minimum radius of source region

For the determination of minimum radius representing a semi-infinite source region, the kerma at 1 m above the ground was calculated with the different radii of source region. The kerma was examined with radius of source region from 1 mfp to 10 mfp. The estimations were performed for twelve energies sources from 10 keV to 5 MeV. Figure 2 shows the relation between the kerma and the source radius for source energies of 10 keV, 100 keV and 5 MeV. It is shown that the radius of source region that is regarded as the semi-infinite source depends strongly on the initial energy of photon. As for the initial energy of 10 keV, the radius of 2.5 mfp can be regarded as a minimum radius of semi-infinite source. On the other hand, at initial energy of 100 keV, a radius of source region has been chosen to be 7 mfp, and at energy of 5 MeV, the minimum radius of source region is about 5 mfp.

Table 4 presents the minimum radius of source region with 12 different energies from 10 keV to 5 MeV. The results are plotted in Fig. 3. From this figure, it can be seen that the minimum radius of source region increases in the energy range from 10 keV to 100 keV and then decreases with increasing energy in the energy region from 100 keV to 5 MeV. In the energy region between 100 keV and 5 MeV, the dominant interaction of photon in air is the Compton scattering. The scattered photons that further penetrate air increase the size of minimum radius regarded as the semi-infinite source in the energy range. The radius of source region in Table 4 was used to define a semi-infinite source region. The relative standard deviations of the kerma calculations were kept less than 1 %.

3.2 Angular Distribution of Photon Fluence

The calculated energy distributions of the photon fluence $\Phi(E)$ at a height of 1 m above the ground are shown in Table 5 for twelve source energies. The relative standard deviations of the calculated values are less than 5 %. The $\Phi(E)$ for the source energies of 2 MeV, 100 keV and 70 keV are presented in Figs. 4 and 5. In the case of the source energies below 70 keV, the energy distribution of the photon is nearly the same as the initial energy. It reflects the small contribution of the scattered radiation, especially, for lower energies. For the initial energy over 100 keV, the photons were assumed to be distributed in the energy range over 30 keV. In Fig. 4, the energy spectrum has a maximal peak in the energy from 70 to 100 keV. In the region of source energy over 100 keV, the shape of energy spectrum does not alter much. In the energy region below 30 keV, the contribution from scattered photons decreases due to the photoelectric absorption.

The calculated angular distributions $\Phi(E, \theta)$ are presented in Fig. 6 for the source energies of 0.05, 0.07, 0.1, 0.2, 1 and 2 MeV. In this figure, the incident directions of photons are defined as cosines to a normal vector to the ground surface. The values of cosine from 1 to −1 (corresponding to the angles from 0 to 180°) were divided to 11 groups with a step of 0.2 radians. This figure shows that the angular distribution is almost isotropic in the energy range below 0.2 MeV.

Figures 7 and 8 present $\Phi(E, \theta)$ for the source energy of 2 MeV. It is found in Fig.7 that the shape of energy spectrum in each angular bin is similar to the $\Phi(E)$ shown in Fig. 4, and the energy spectra have a peak in the energy region from 70 to 100 keV. The shapes of the angular distribution to the energy bins in Fig. 8 is similar to those in Fig. 6. It means that for the low energy bins, the angular distributions are nearly uniform for the incident directions of the photon, especially, in the energy bins less than 100 keV. However, in the higher energy bins, the number of photons increases with increasing the cosine.

3.3 Organ Doses and Effective Doses for Mono-energetic Sources

The calculated organ doses for the phantoms: newborn, 1, 5, 10 and 15 years, and adult due to semi-infinite sources at twelve energies from 10 keV to 5 MeV are presented in Tables 6 to 11. The statistical error of calculation is less than 10 % for energies above 30 keV. For lower energies and smaller organs, especially for energies of 15 and 10 keV, the calculation of the deep-lying organ doses was not carried out, since low energy photons did not reach these organs.

The comparison of organ doses in adult between the present work and FGR-12[8] indicates a good agreement, and difference is less than 10 % (the difference is less than 5 % in almost of data) for photon energies above 200 keV. In energy region from 50 to 200 keV, the difference is less than 15 %. In the lower energy photons, almost all data are good agreement, but some data are not as good agreement (difference is between 20 to 30%). Moreover, for all obtained results of organ doses in this work are lower than the results from FGR-12. The reason of this difference can be due to the difference of calculation method as discussion below.

Table 12 gives the values of the effective dose E calculated for six age groups. The conversion coefficients of the effective dose normalized to unit air kerma in free air for these age groups were presented in Table 13 and Fig. 9. From Tables 12 and 13 and Fig. 9, it can be seen that the effective doses depend upon the body size; the effective doses in younger phantom are higher than those in the older phantoms, especialy below 100 keV. The main reason is the shielding effect of the body. The bigger body has a higher shielding effect and

the lower energy photons do not reach the organs. Therefore, the organs in the bigger body receive lower doses.

Figure 10 presents the ratios of the effective doses in different phantoms to the effective dose of adult phantom. From Fig. 10 and Table 12, it can be seen that the difference in the effective dose between the adult and the 15-years phantoms is less than 2 % in the energy region above 100 keV and below 12 % at energy of 10 keV. It also shows that the dependence of doses on the body size is more pronounced in the energy region below 100 keV. For example, the defference of effective dose between the adult and the newborn phantoms is about 10 times at 10 keV and less than 1.35 times above 100 keV, while the difference between the adult phantom and the 5-years phantom is about 4.2 times and less than 1.21 times. The organ dose and effective dose at low photon energies are sensitive to the organ position and the body size. The similar conclusion can be also found in the previous studies.[15, 26,27)]

The effective doses for the adult phantom are also compared to those from FGR-12[8)] and Zankl *et al.*[9)] in Fig. 11. The calculated effective doses in this work show a good agreement with those of FGR-12 and of Zankl *et al.* In the energy above 50 keV, the present data have an excellent agreement with data of Zankl *et al.* and the differences are less than 4 %. However, in the energy below 30 keV, the differences in both data sets are about from 10 to 30 %. It is found that the present results are in quite good agreement with those of FGR-12. However, the present data are lower than those of FGR-12 in all energy regions. A possible reason is the difference in the calculation method for photon spectra from semi-infinite cloud sources; the present data were calculated by the Monte Carlo method, while those of FGR-12 were calculated by the deterministic method.

3.4 Conversion Coefficients of Effective Dose for Radionuclides

Table 14 shows age-dependent conversion coefficients of effective dose for 160 radionuclides distributed in air using the decay data of DECDC. These are significant radionuclides in safety assessment of nuclear facilities.[28)] In Table 14, the conversion coefficients for adult listed in FGR-12 are also shown as reference values. There is good agreement between the present work and FGR-12 on the conversion coefficients for adult. However, the present data are lower than those of FGR-12 for all radionuclides. The difference is about 5 % for the radionuclides that emit dominantly high-energy photons above 100 keV, and less than 10 % for the radionuclides which emit lower energy photons. This is supported by the fact that the calculated effective doses from the mono-energetic photon sources are about 5 % lower than those of FGR-12 at energies above 100 keV, and 5 % more at energies below 100 keV (see Fig. 11). It affects the results in the calculation of conversion coefficient of effective dose for radionuclides.

4. Conclusions

Age-dependent dose conversion coefficients were calculated for external exposure to photon emitters uniformly distributed in air. Organ doses and effective doses were calculated with a series of age-specific MIRD-5 type phantoms using the MCNP code for semi-infinite mono-energetic photon sources of twelve energies from 10 keV to 5 MeV. Based on the result, effective dose conversion coefficients were calculated for 160 radionuclides, which are important for safety assessment of nuclear facilities. The energies and intensities of photons emitted from the radionuclides were taken from the latest decay data DECDC developed at JAERI. The coefficients were tabulated for 6 age groups: newborn, 1, 5, 10 and 15 years, and adult. The effective dose conversion coefficients presented in this report will be used for dose assessment relevant to photon exposure of the member of public around nuclear facilities.

Acknowledgments

The authors would like to thank MEXT Nuclear Research Exchange Program of Japan for the consistent support for this work.

References

1. ICRP. 1990 Recommendations of the International Commission on Radiological Protection. ICRP Publication 60 (1991).
2. ICRU. Determination of dose equivalents resulting from external radiation sources. ICRU Report 39 (1985).
3. Beck, H. L. and de Planque, G. The radiation field in air due to distributed gamma ray source in ground. USAEC Report HASL-195 (1968).
4. Beck, H. L., DeCompo, J. and Gogolak, C. In-situ Ge(Li) and Na(Tl) gamma ray spectrometry. USAEC Report HASL-258 (1972).
5. Kocher, D. C. and Sjoreen, A. L. Dose rate conversion factors for external exposure to photon emitters in soil. Health Phys., 48,193-205 (1985).
6. Chen, S. Y. Calculation of effective dose-equivalent responses for external exposure from residual photon emitters in soil. Health Phys., 60, 411-426 (1991).
7. Saito, K. and Jacob, P. Gamma ray fields in the air due to sources in the ground. Radiat. Prot. Dosim., 58, 29-45 (1995).
8. Eckerman, K. F. and Ryman, J. C. External exposure to radionuclides in air, water, and soil. Federal Guidance Report No.12. EPA-402-R-93-81 (1993).
9. Zankl, M., Petoussi, N. and Drexler, G. Effective dose and effective dose equivalent - the impact of the new ICRP definition for external photon irradiation. Health Phys., 62, 395-399 (1992).
10. Saito, K. and Moriuchi, S. Development of a Mote Carlo code for the calculation of gamma ray transport in the natural environment. Radiat. Prot. Dosim., 12, 21-28 (1985).
11. Yamaguchi, Y. and Yoshizawa, M. Calculation of effective dose for external photon exposure based on ICRP new recommendations. Proc. IV Int. Cong. Radiat. Prot. Soc., 485-495, Salamanca, Spain (1991).
12. Yamaguchi, Y. and Yoshizawa, M. Angular dependence of organ doses and effective dose for external photon irradiation. Proc. 8th Int. Cong. Radiat. Prot. Assoc., 123-124, Montreal, Canada (1992).
13. Yamaguchi, Y. DEEP code to calculate dose equivalents in human phantom for external photon exposure by Monte Carlo method. JAERI-M 90-235 (1990).
14. Yamaguchi, Y. Age-dependent effective dose for external photons. Radiat. Prot. Dosim., 55, 123-129 (1994).
15. Clouvas, A., Xanthos, S., Antonopoulos-Domis, M. and Silva, J. Monte Carlo calculation of dose rate conversion factors for external exposure to photon emitters in soil. Health Phys., 78, 295-302 (2000).
16. Briesmeister, J. F., Ed. MCNP-A general Monte Carlo N-particle transport code Version 4B. LA-12625-M (1997).
17. Hubbell, L. H., Veigele, W. J., Briggs, E. A., Brown, R. T., Cromer, D. T. and Howerton, R. J. Atomic form factors, incoherent scattering functions and photon scattering cross sections. J. Phys. Chem. Ref. Data 4, 471 (1975).
18. Everett, C. J. and Cashwell, E. D. MCNP code fluorescence-routine revision. LA-5240-MS (1973).
19. Eckerman, K. F., Cristy, M. and Ryman, J. C. The ORNL mathematical phantom series. Oak Ridge National Laboratory Report, available at http://homer.hsr.ornl.gov/VLab/VLabPhan.html (1996).
20. Cristy, M. and Eckerman, K.F. Specific absorbed fractions of energy at various ages from internal photon sources, I. Methods. ORNL/TM-8381/V1 (1987).

21. Snyder, W. S., Ford, M. R., Warner, G. G. and Watson, S. B. A tabulation of dose equivalent per microcurie-day for source and target organs of adult for various radionuclides: Part 1. ORNL-5000 (1974).
22. ICRP. Conversion coefficients for use in radiological protection against external radiation. ICRP Publication 74 (1995).
23. Roesch, W.C. US-Japan joint reassessment of atomic bomb radiation dosimetry in Hiroshima and Nagasaki: Final report. Radiation Effects Research Foundation (1987).
24. Hubbell, J. H., Photon mass attenuation and energy absorption coefficients from 1 keV to 20 MeV. Int. J. Appl. Radiat. Isot., 33, 1269-1290 (1982) .
25. Endo, A. and Yamaguchi, Y. Complilation of new nucler decay data files used for dose calculation. J. Nucl. Sci. Technol., 38, 689-696 (2001).
26. Saito, K., Petoussi-Henss, N. and Zankl, M. Calculation of the effective dose and its variation from environmental gamma ray sources. Health Phys., 74, 698-706 (1998).
27. Petoussi, N., Jacob, P., Zankl, M. and Saito, K. Organ doses for foetuses, babies, children and adults from environmental gamma rays. Radiat. Prot. Dosim., 37, 31-41 (1991).
28. Nuclear Safety Comission, Ed. Guidelines for Safety Assessment of Nuclear Safety Comission, 10th Edition. Taisei Publishing (2000).

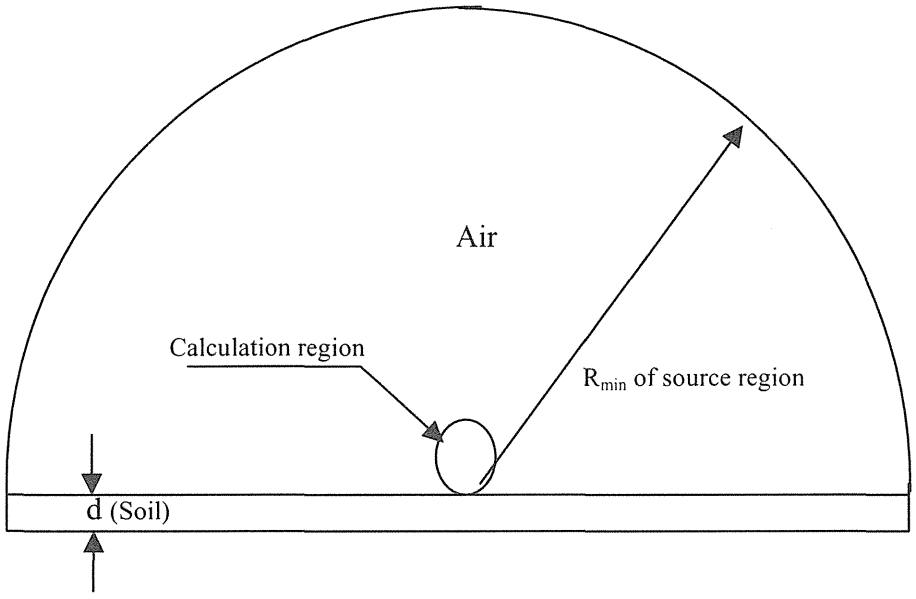

Fig. 1. Geometry of computational model.

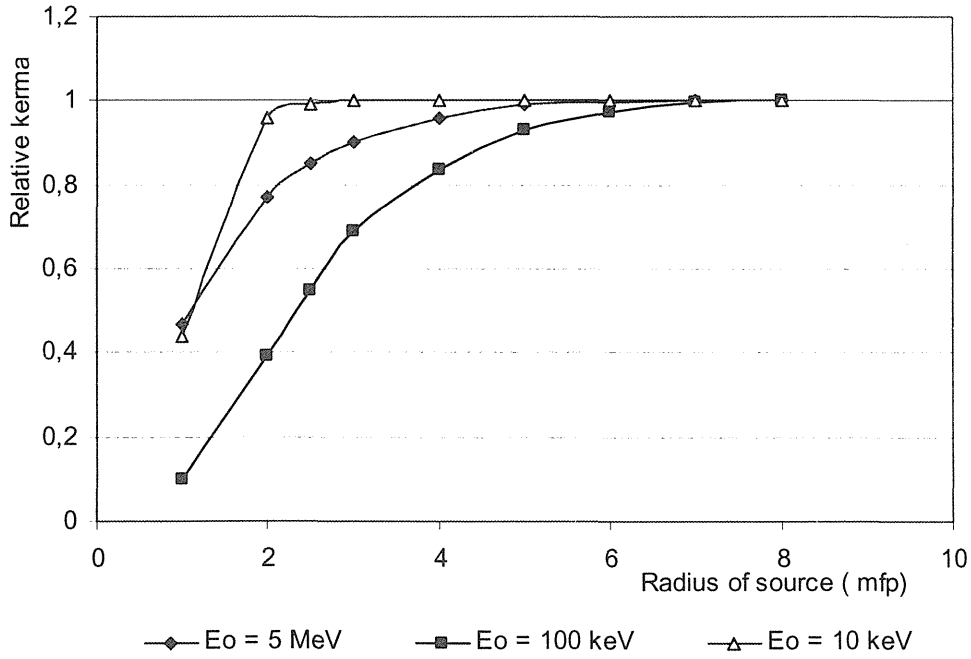

Fig. 2 Relation of relative kerma and the radius of source.

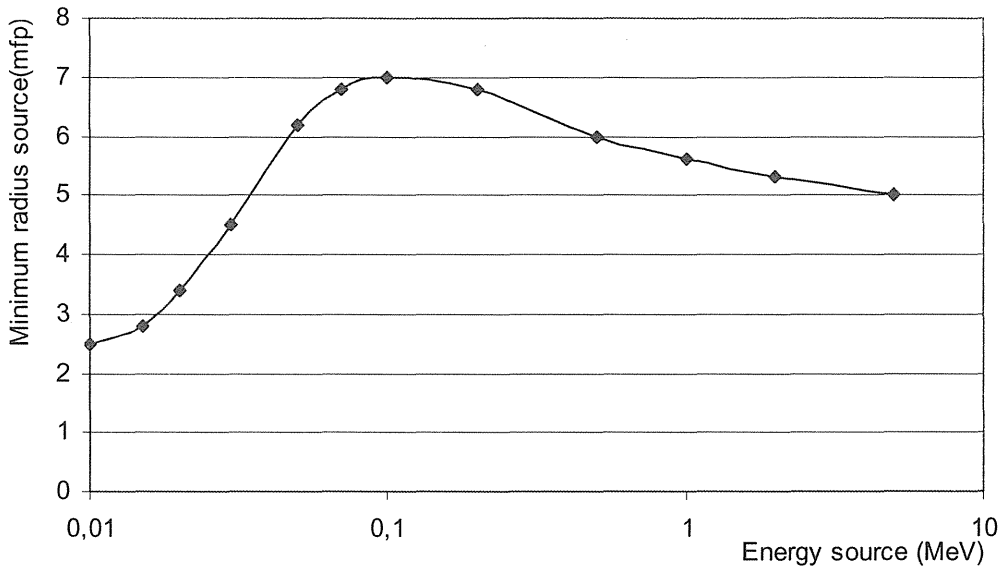

Fig. 3 Minimum radius of the source region as a function of source energies.

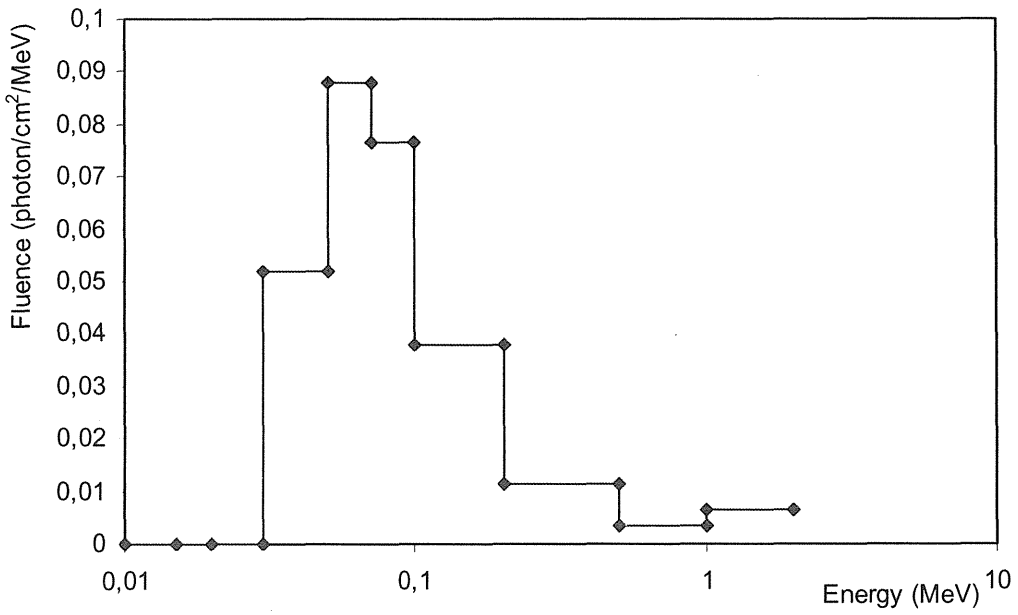

Fig. 4 Energy distribution of photon fluence at 1 m above the ground with source energy of 2 MeV.

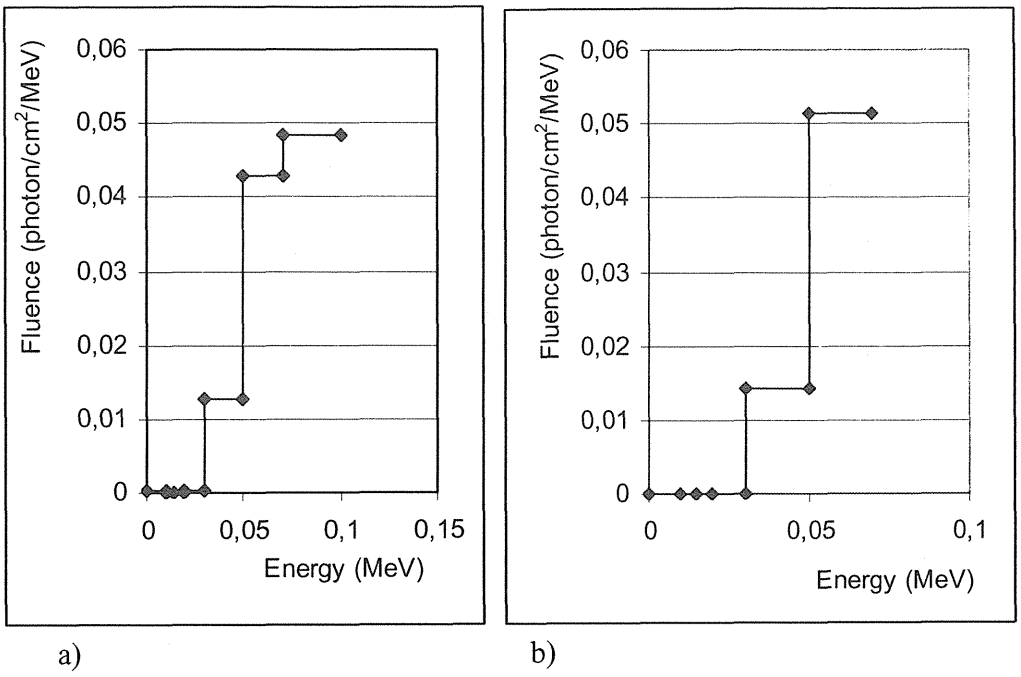

a) b)

Fig. 5 Energy distribution of photon fluence at 1 m above the ground with source energies: a) 100 keV and b) 70 keV.

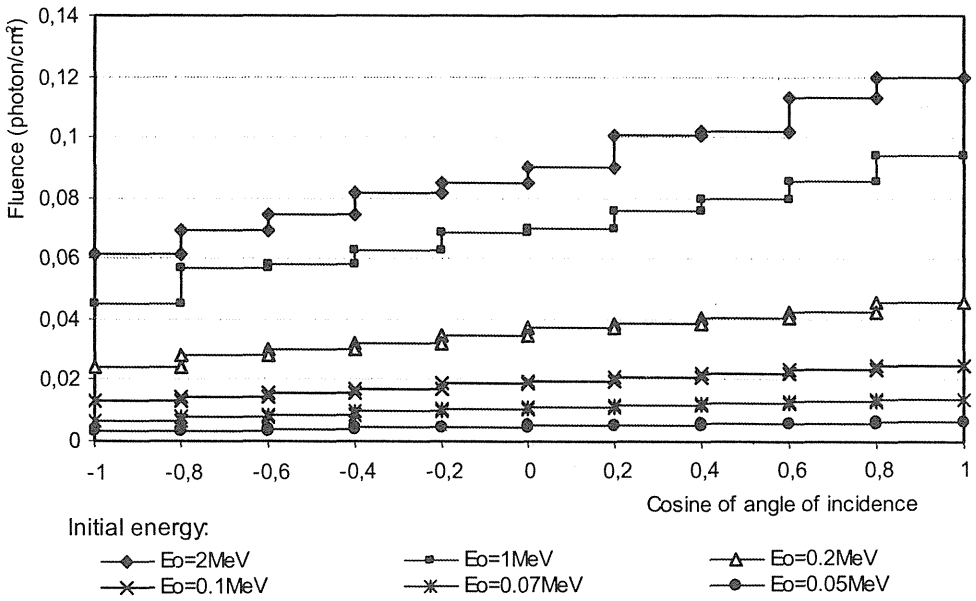

Fig. 6 Angular distribution of several source energies.

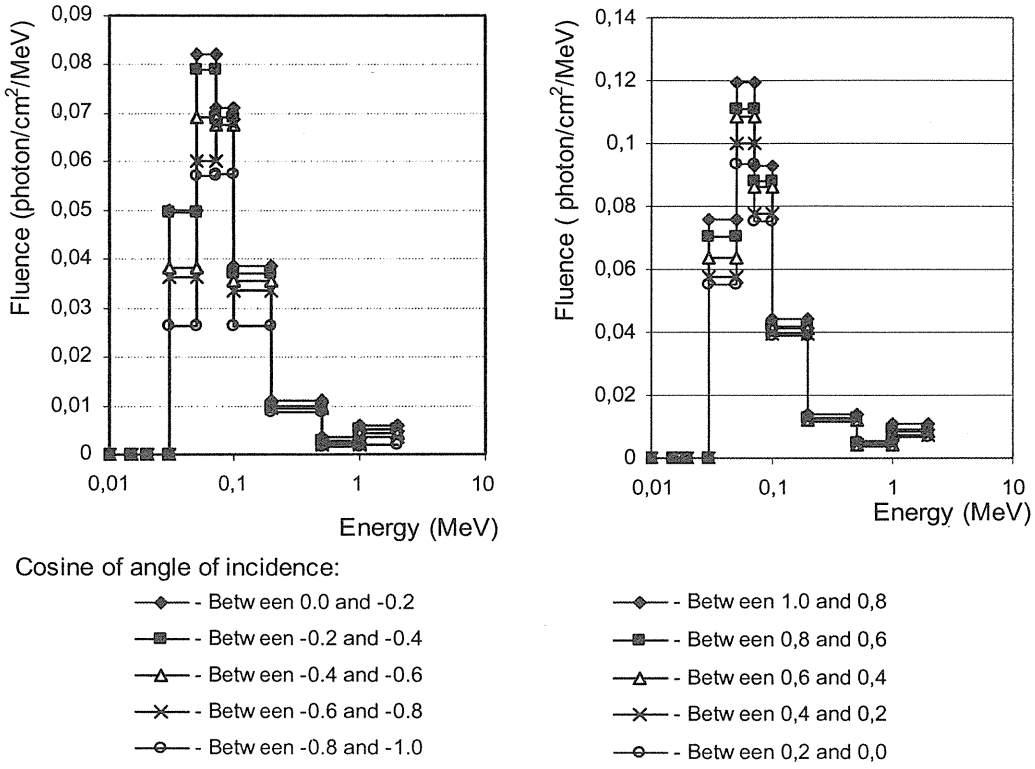

Fig. 7 Energy distribution to angular bins of the photon fluences with source energy of 2 MeV.

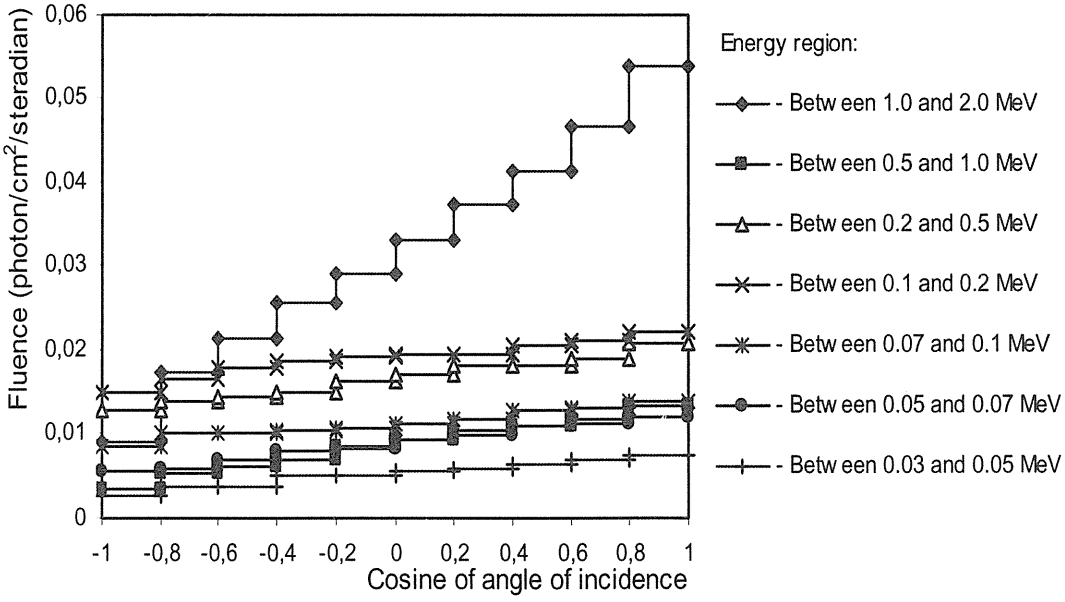

Fig. 8 Angular distribution to energy bins of the fluences with source energy of 2 MeV.

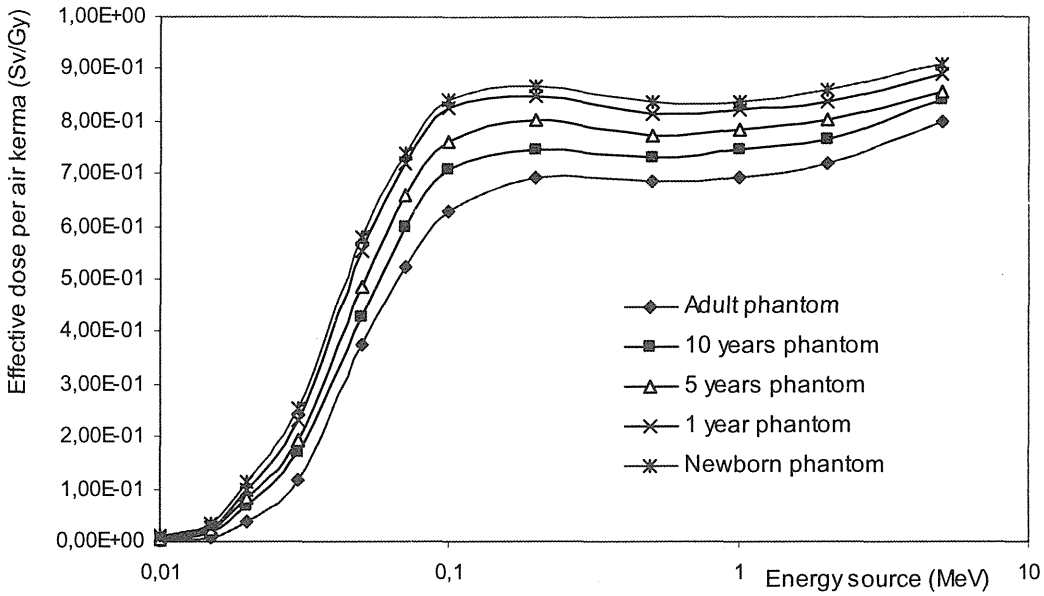

Fig 9. Variation of the effective dose due to age for a semi-infinite source in the air.

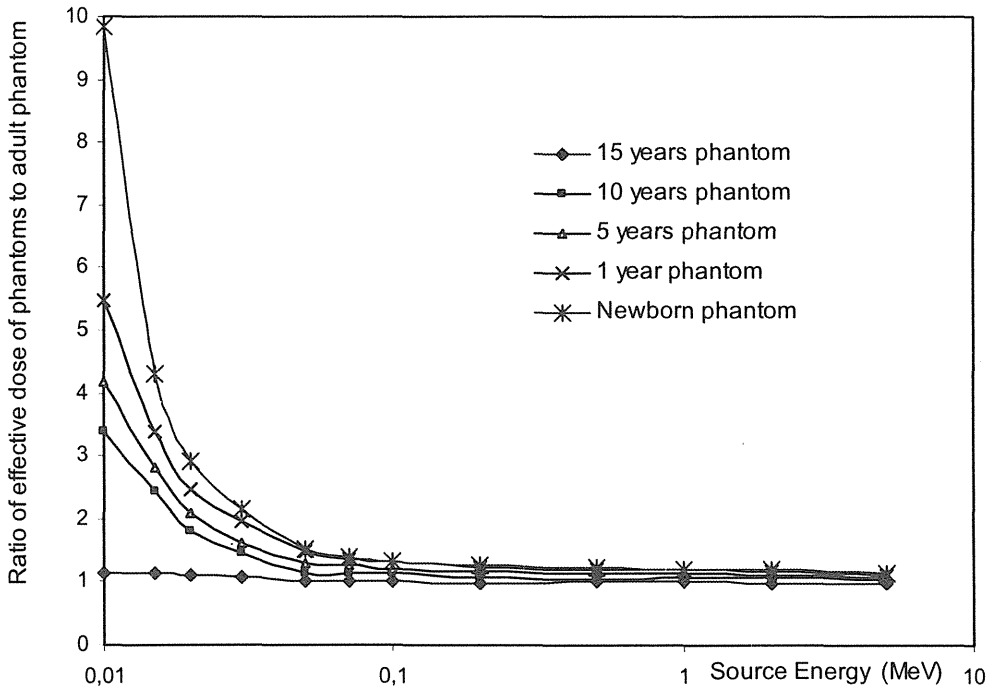

Fig.10 Ratio of the effective doses of age-specific phantoms to those of adult phantom.

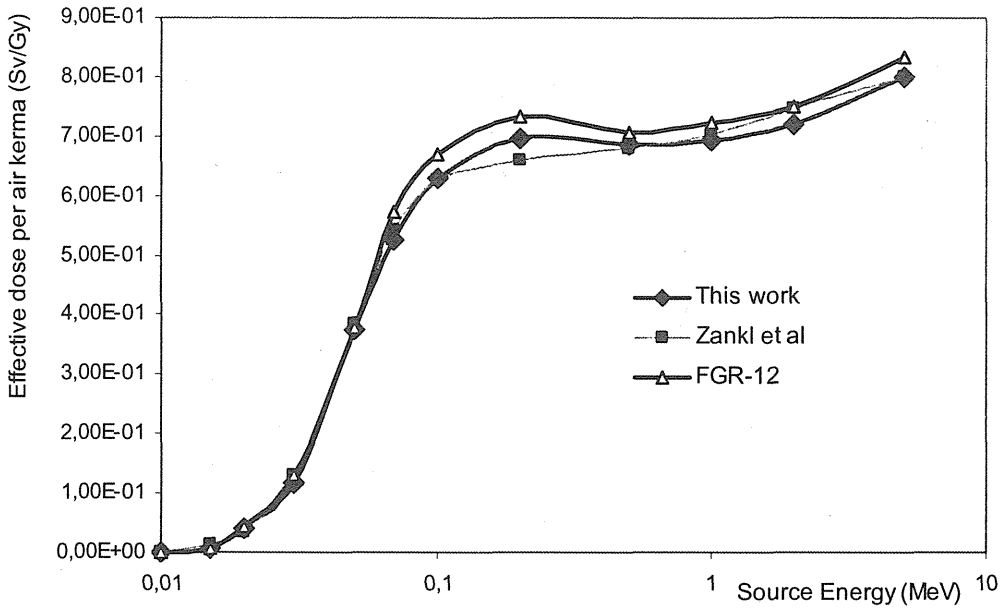

Fig. 11 Effective dose per air kerma for adult phantom for a semi-infinite source in the air.

Table 1 Elemental compositions of the tissues for phantoms (percent by weight)

	All phantoms except newborn			Newborn		
Element	Soft tissue	Skeleton	Lung	Soft tissue	Skeleton	Lung
H	10.454	7.337	10.134	10.625	7.995	10.134
C	22.663	25.475	10.238	14.964	9.708	10.238
N	2.490	3.057	2.866	1.681	2.712	2.866
O	63.525	47.893	75.752	71.830	66.811	75.752
F	0	0.025	0			
Na	0.112	0.326	0.184	0.075	0.314	0.184
Mg	0.013	0.112	0.007	0.019	0.143	0.007
Si	0.030	0.002	0.006			
P	0.134	5.095	0.080	0.179	3.712	0.080
S	0.204	0.173	0.225	0.240	0.314	0.225
Cl	0.133	0.143	0.266	0.079	0.140	0.266
K	0.208	0.153	0.194	0.301	0.148	0.194
Ca	0.024	10.190	0.009	0.003	7.995	0.009
Fe	0.005	0.008	0.037	0.004	0.008	0.037
Zn	0.003	0.005	0.001			
Rb	0.001	0.002	0.001			
Sr	0	0.003	0			
Zr	0.001	0	0			
Pb	0	0.001	0			
Density (g cm^{-3})	1.04	1.4	0.296	1.04	1.22	0.296

Table 2 Air and soil composition used in calculation

Air Composition		Soil Composition	
Element	Mass Fraction	Element	Mass Fraction
H	0.00064	H	0.021
C	0.00014	C	0.016
N	0.75086	O	0.577
O	0.23555	Al	0.050
Ar	0.01281	Si	0.271
		K	0.013
		Ca	0.041
		Fe	0.011
Total	1.0000	Total	1.000

Table 3 Mass attenuation coefficients μ'/ρ and mfp for photons in air and a soil used in this calculation

Energy (MeV)	Air		Soil	
	μ'/ρ (cm^2 g^{-1})	mfp (m)	μ'/ρ (cm^2 g^{-1})	mfp (cm)
0.010	4.748	1.75	20.3	0.0302
0.015	1.432	5.80	6.161	0.0999
0.02	0.6754	12.3	2.586	0.238
0.03	0.3104	26.7	0.8815	0.698
0.04	0.2251	36.9	0.4601	1.34
0.05	0.1935	42.9	0.3119	1.97
0.06	0.1777	46.7	0.2458	2.50
0.08	0.1609	51.6	0.1902	3.24
0.10	0.1507	55.1	0.1667	3.69
0.15	0.1341	61.9	0.1403	4.39
0.2	0.1225	67.7	0.1263	4.87
0.3	0.1063	78.1	0.1088	5.66
0.4	0.0952	87.2	0.0972	6.33
0.5	0.0869	95.5	0.0887	6.94
0.6	0.0804	103	0.0820	7.50
0.662	0.0770	108	0.0785	7.84
0.8	0.0706	118	0.0720	8.55
1.0	0.0635	131	0.0647	9.51
1.25	0.0568	146	0.0579	10.6
1.5	0.0517	161	0.0527	11.7
2.0	0.0444	187	0.0454	13.6
3.0	0.0354	234	0.0361	17.0
4.0	0.0307	270	0.0320	19.2
5.0	0.0275	302	0.0290	20.6
6.0	0.0251	331	0.0267	23.0
8.0	0.0221	376	0.0240	25.6
10.0	0.0204	407	0.0227	27.1

Table 4 Determined minimum radius of source region for twelve source energies

Initial energy of source (MeV)	Minimum radius (mfp)
0.01	2.5
0.015	2.8
0.02	3.2
0.03	4.5
0.05	6.2
0.07	6.8
0.10	7.0
0.20	6.8
0.50	6.0
1.00	5.6
2.00	5.3
5.00	5.0

Table 5 Calculated energy distribution Φ(E) for 12 source energies

Energy (MeV)	5MeV	2MeV	1MeV	0.5MeV	0.2MeV	0.1MeV
0.01	2.16e-7(50)	3.65e-7 (37)	2.87e-7(57)	3.33e-7(60)	9.81e-8(62)	1.53e-8(36)
0.015	5.27e-7(60)	6.75e-7 (31)	1.84e-6(71)	2.05e-7(47)	2.65e-9(68)	3.46e-9(49)
0.02	4.26e-7(55)	8.65e-7 (35)	5.17e-7(23)	1.13e-6(83)	3.29e-8(34)	1.39e-7(80)
0.03	2.65e-6(40)	2.67e-5 (24)	6.24e-5(20)	3.06e-5(7)	3.02e-5(7)	3.79e-5(7)
0.05	1.20e-3(10)	1.31e-3 (4.5)	2.13e-3(4.8)	1.62e-3(3)	1.60e-3(1.7)	1.96e-3(1.2)
0.07	3.54e-3(3)	3.09e-3 (3.7)	3.59e-3(3)	3.57e-3(5)	3.16e-3(1.5)	3.81e-3(0.7)
0.10	4.75e-3(2)	3.99e-3 (2.8)	4.23e-3(2)	4.15e-3(2)	4.15e-3(1.4)	7.35e-3(0.6)
0.20	9.20e-3(1.5)	7.34e-3 (2.7)	7.22e-3(2)	7.61e-3(3)	1.03e-2(0.66)	
0.50	8.58e-3(1.5)	6.76e-3 (2.9)	6.28e-2(2)	1.08e-2(1)		
1.00	4.12e-3(1)	3.44e-3 (2.9)	1.02e-2(0.9)			
2.00	2.75e-3(1)	1.26e-2 (0.7)				
5.00	1.77e-2(0.5)					
TT	5.19e-2(1)	3.86e-2 (1)	3.37e-2(1.4)	2.78e-2(1.4)	1.92e-2(0.62)	1.32e-2(0.7)

(*) The values in brackets are relative errors. TT is total photon fluence
- The value of 5.19e-2(1) is 5.19×10^{-2} with the relative error of 1%

Table 5 - continued

Energy (MeV)	0.07MeV	0.05MeV	0.03MeV	0.02MeV	0.015MeV	0.01MeV
0.01	1.64e-8(27)	2.59e-8(17)	6.08e-8(24)	6.52e-8(17)	5.31e-8(11)	1.44e-4(0.5)
0.015	2.98e-9(39)	1.34e-8(50)	1.23e-9(26)	3.04e-9(40)	4.16e-4(0.6)	
0.02	1.09e-7(67)	9.99e-9(22)	9.94e-8(14)	6.62e-4(1)		
0.03	4.53e-5(4.2)	7.97e-5(4)	2.38e-3(0.6)			
0.05	2.57e-3(0.7)	6.22e-3(0.8)				
0.07	6.96e-3(0.5)					
TT	9.57e-3(0.43)	6.30e-3(0.8)	2.38e-3(0.6)	6.62e-4(1)	4.17e-4(0.6)	1.44e-4(0.5)

(*) The values in brackets are relative errors. TT is total photon fluence

Table 6 Organ doses calculated using MCNP code with phantom of newborn due to semi-infinite source at twelve energies from 0.01 to 5 MeV (Gy per Bq s m^{-3})

Organ	5 MeV (10^{-13})	2MeV (10^{-13})	1MeV (10^{-14})	0.5MeV (10^{-14})	0.2 MeV (10^{-15})	0.1MeV (10^{-15})	0.07MeV (10^{-15})
Adrenals	3.18(4)	1.05(2)	5.30(3)	2.66(4)	8.82(1)	3.84(2)	2.60(3)
B surface	3.34(1)	1.32(4)	7.75(3)	4.21(3)	29.7(2)	25.7(3)	19.7 (2)
Brain	3.30(1)	1.29(2)	5.80(2)	3.02(2)	11.2(2)	4.82(1)	3.05(1)
Breasts	3.02(1)	1.20(5)	5.44(3)	2.81(7)	11.1 (6)	4.35(4)	3.51(4)
Esophagus	3.09(2)	1.09(2)	5.42(3)	2.58(3)	11.1 (8)	4.19(4)	2.60(4)
ST wall	2.90(1)	1.08(2)	5.33(3)	2.56(4)	9.30(4)	4.10(3)	2.88(3)
SI wall	3.00(1)	1.14(2)	4.87(1)	2.60(4)	9.17(4)	4.10(4)	2.56(2)
ULI wall	2.97(2)	1.16(3)	5.03(2)	2.57(4)	9.10(8)	3.79(3)	2.45(2)
LLI wall	2.88(2)	1.09(2)	4.88(2)	2.59(4)	8.84(4)	4.42(8)	2.55(2)
G. Bladder	2.89(2)	1.06(2)	4.95(2)	2.60(4)	9.74(8)	4.10(3)	2.35(3)
Heart	3.10(2)	1.10(2)	5.42(3)	2.54(2)	9.67(3)	4.53(5)	2.74(1)
Kidneys	3.06(3)	1.10(1)	5.35(3)	2.59(3)	9.79(5)	4.45(2)	2.76(1)
Liver	3.03(1)	1.17(1)	5.19(1)	2.51(2)	9.98(3)	4.49(7)	2.74(1)
Lung	3.17(1)	1.19(1)	5.68(1)	2.66(1)	10.6(6)	4.99(2)	3.03(1)
Muscle	3.16(1)	1.19(2)	5.78(2)	2.71(2)	9.67(1)	4.86(3)	3.14(1)
Ovaries	2.88(3)	1.09(6)	4.74(3)	2.16(6)	8.33	3.58(5)	2.51(5)
Pancreas	2.89(3)	1.07(3)	4.82(3)	2.18(2)	9.02(4)	3.93(3)	2.41(2)
Bone R	3.22(1)	1.29(4)	6.10(2)	2.85(2)	10.9(1)	5.12(2)	2.96(2)
Skin	2.89(1)	1.12(2)	5.53(2)	2.60(1)	10.3 (5)	5.32(2)	3.61(1)
Spleen	2.96(1)	1.12(2)	5.27(2)	2.54(3)	8.81(3)	4.33(6)	2.69(2)
Testes	2.90(3)	1.10(5)	4.94(4)	2.57(3)	9.81(3)	4.98(8)	3.08(5)
Thymus	3.12(2)	1.18(2)	5.40(4)	2.44(2)	9.88(4)	4.43(5)	3.09(5)
Thyroid	2.88(2)	1.08(3)	5.01(2)	2.72(4)	11.1 (5)	4.12(4)	2.80(4)
U bladder	3.28(8)	1.03(2)	4.84(2)	2.40(5)	9.78(6)	4.01(5)	2.75(3)
Uterus	2.82(1)	1.06(2)	4.77(3)	2.22(6)	8.51(4)	3.36(2)	2.41(3)
E	3.03	1.15	5.38	2.64	10.3	4.77	3.08

(*) The values in brackets are relative errors

Table 6 - continued

Organ	0.05MeV (10^{-15})	0.03MeV (10^{-16})	0.02MeV (10^{-17})	0.015MeV	0.01MeV
Adrenals	1.66(4)	4.75(4)	6.95(2)	7.10e-18(3)	-
B surface	12.6 (2)	48.3(1)	120(1)	36.7e-16(1)	2.60e-17(1)
Brain	2.27(3)	7.52(1)	13.2(1)	1.94e-17(1)	9.11e-20(2)
Breasts	2.30(7)	10.4 (3)	64.0(2)	4.53e-16(2)	1.67e-16(3)
Esophagus	1.63(4)	4.54(8)	3.33(3)	9.07e-19(7)	-
ST wall	1.83(4)	4.82(2)	7.91(1)	7.99e-18(2)	-
SI wall	1.52(2)	3.88(2)	3.70(2)	1.33e-18(2)	-
ULI wall	1.61(5)	4.14(2)	5.37(3)	2.77e-18(3)	-
LLI wall	1.47(2)	4.05(5)	3.59(2)	1.34e-18(4)	-
G. Bladder	1.52(3)	4.24(8)	3.34(4)	7.90e-19(9)	-
Heart	1.76(2)	5.20(3)	6.72(1)	5.62e-18(1)	2.76e-20(8)
Kidneys	1.70(4)	5.27(2)	11.9(2)	1.94e-17(1)	1.36e-19(7)
Liver	1.82(2)	5.40(3)	9.19(1)	1.17e-17(1)	6.78e-20(4)
Lung	1.99(2)	6.70(3)	12.6(4)	1.31e-17(1)	4.59e-20(6)
Muscle	1.87(1)	7.10(2)	23.2(1)	8.94e-17(1)	1.74e-17(1)
Ovaries	1.36(4)	3.03(4)	1.78(8)	1.79e-19(25)	-
Pancreas	1.48(3)	4.39(2)	2.41(3)	2.77e-19(9)	-
Bone R	1.69(2)	5.99(1)	15.8(1)	5.20e-17(1)	4.06e-18(1)
Skin	2.40(3)	10.0(1)	60.9(1)	4.49e-16(1)	2.65e-16(1)
Spleen	1.71(3)	4.93(2)	7.68(2)	6.58e-18(6)	5.10e-21(25)
Testes	1.76(4)	6.40(7)	18.2(3)	6.94e-17(1)	1.19e-17(4)
Thymus	2.09(7)	6.87(2)	15.6(1)	2.68e-17(1)	2.21e-19(7)
Thyroid	1.69(4)	6.01(4)	15.3(2)	5.28e-17(2)	5.15e-18(4)
U bladder	1.66(5)	5.42(8)	7.74(2)	7.54e-18(2)	3.98e-10(30)
Uterus	1.37(5)	3.28(3)	2.43(3)	3.75e-19(9)	-
E	1.90	6.01	15.8	5.64e-17	1.45e-17

(*) The values in brackets are relative errors
- The value of 7.10e-18(3) is 7.10×10^{-18} with the relative error of 3%.

Table 7 Organ doses calculated using MCNP code with phantom of 1 year due to semi-infinite source at twelve energies from 0.01 to 5 MeV (Gy per Bq s m^{-3})

Organ	5 MeV (10^{-13})	2MeV (10^{-13})	1MeV (10^{-14})	0.5MeV (10^{-14})	0.2 MeV (10^{-15})	0.1MeV (10^{-15})	0.07MeV (10^{-15})
Adrenals	2.80(2)	1.06(2)	5.09(3)	2.45(3)	8.73(3)	3.79(2)	2.53(4)
B surface	3.43(3)	1.34(1)	7.73(2)	4.84(2)	30.5(1)	24.2(2)	19.3(2)
Brain	3.06(1)	1.15(1)	5.28(1)	2.65(1)	10.3(2)	4.63(1)	2.95(1)
Breasts	3.11(3)	1.15(3)	5.65(3)	2.81(5)	10.1(4)	5.31(4)	3.42(4)
Esophagus	2.86(2)	1.06(1)	4.96(2)	2.32(2)	8.75(3)	4.11(3)	2.53(5)
ST wall	2.90(1)	1.08(1)	5.15(3)	2.56(3)	9.85(4)	4.38(2)	2.81(3)
SI wall	2.88(2)	1.06(1)	4.97(1)	2.39(1)	9.29(2)	4.16(2)	2.51(1)
ULI wall	2.81(1)	1.09(2)	4.96(2)	2.40(1)	9.64(7)	4.13(2)	2.38(2)
LLI wall	2.84(1)	1.09(2)	5.04(1)	2.46(2)	9.14(3)	4.35(2)	2.52(2)
G. Bladder	2.84(4)	1.02(2)	4.70(2)	2.27(3)	8.79(3)	4.00(3)	2.29(3)
Heart	2.86(1)	1.08(1)	4.99(2)	2.51(2)	9.47(2)	4.50(2)	2.69(1)
Kidneys	2.89(1)	1.08(1)	5.15(2)	2.50(2)	9.33(2)	4.38(3)	2.71(1)
Liver	2.91(2)	1.09(1)	5.17(1)	2.58(2)	9.73(2)	4.44(2)	2.68(1)
Lung	3.00(2)	1.15(1)	5.50(1)	2.71(2)	10.4(2)	4.90(1)	3.00(1)
Muscle	3.13(2)	1.16(1)	5.64(1)	2.70(1)	10.3(1)	4.78(1)	3.08(1)
Ovaries	2.69(3)	1.06(3)	4.64(4)	2.31(3)	8.23(8)	3.50(4)	2.46(5)
Pancreas	2.68(2)	1.04(2)	4.69(3)	2.26(2)	8.18(2)	3.99(2)	2.37(1)
Bone R	3.19(3)	1.17(1)	5.83(2)	2.69(1)	10.2(1)	4.62(1)	2.89(2)
Skin	3.27(2)	1.24(1)	6.09(1)	2.98(1)	11.3(1)	5.36(1)	3.54(1)
Spleen	2.88(1)	1.09(1)	5.14(2)	2.80(8)	9.12(2)	4.28(2)	2.62(2)
Testes	2.93(4)	1.13(3)	4.88(4)	2.40(3)	9.71(5)	4.85(3)	3.03(4)
Thymus	3.00(1)	1.09(1)	5.41(2)	2.66(2)	9.76(2)	4.91(4)	3.09(4)
Thyroid	2.83(2)	1.07(2)	5.51(4)	2.52(3)	10.8(5)	4.10(2)	2.73(4)
U bladder	2.86(2)	1.06(3)	5.94(2)	2.45(3)	9.10(2)	4.23(3)	2.67(2)
Uterus	2.91(3)	1.01(2)	4.41(3)	2.39(3)	8.47(3)	3.68(4)	2.35(2)
E	2.96	1.12	5.25	2.57	10.0	4.68	3.01

(*) The values in brackets are relative errors

Table 7 - continued

Organ	0.05MeV (10^{-15})	0.03MeV (10^{-16})	0.02MeV (10^{-17})	0.015MeV	0.01MeV
Adrenals	1.35(3)	2.71(4)	2.38(4)	8.14e-19(14)	-
B surface	12.9(2)	38.8(2)	71.2(2)	14. 9e-17(1)	7.43e-18(1)
Brain	1.85(1)	4.57(3)	4.34(1)	2.40e-18(1)	7.51e-22(15)
Breasts	2.32(8)	11.4(7)	57.3(4)	3.07e-16(2)	7.18e-17(3)
Esophagus	1.37(5)	2.37(3)	0.97(4)	1.62e-19(14)	-
ST wall	1.72(4)	4.01(4)	4.85(4)	3.54e-18(3)	4.33e-21(40)
SI wall	1.40(3)	2.44(2)	1.33(2)	3.29e-19(3)	-
ULI wall	1.46(4)	2.84(2)	2.18(2)	7.43e-19(7)	-
LLI wall	1.39(3)	2.65(2)	1.44(4)	3.52e-19(11)	-
G. Bladder	1.49(8)	2.58(4)	1.12(4)	1.60e-19(17)	-
Heart	1.75(3)	3.63(2)	2.98(1)	1.80e-18(2)	4.95e-21(16)
Kidneys	1.64(3)	4.55(2)	7.49(2)	8.76e-18(2)	2.53e-20(8)
Liver	1.79(4)	4.03(2)	4.57(2)	3.57e-18(1)	5.14e-21(14)
Lung	1.95(3)	5.04(2)	5.94(1)	4.09e-18(1)	5.87e-21(12)
Muscle	2.00(1)	6.46(1)	18.2(1)	5.90e-17(1)	8.74e-18(1)
Ovaries	1.29(6)	1.88(4)	0.49(8)	-	-
Pancreas	1.38(5)	2.28(3)	0.71(4)	3.63e-20(20)	-
Bone R	1.68(2)	4.56(2)	7.70(1)	15.5e-18(1)	8.07e-19(1)
Skin	2.53(1)	11.8(1)	61.2(1)	3.81e-16(1)	1.85e-16(1)
Spleen	1.50(3)	3.92(3)	3.83(3)	1.84e-18(4)	-
Testes	1.73(9)	7.08(3)	26.5(2)	1.04e-16(3)	1.12e-17(3)
Thymus	1.97(4)	5.12(2)	7.72(1)	7.64e-18(3)	1.94e-20(15)
Thyroid	1.71(5)	5.73(8)	13.5(2)	4.11e-17(2)	3.08e-18(7)
U bladder	1.72(3)	4.09(4)	4.62(2)	3.41e-18(3)	-
Uterus	1.24(4)	1.98(4)	0.71(7)	-	-
E	1.84	5.45	13.3	4.71e-17	8.05e-18

(*) The values in brackets are relative errors
- The value of 8.14e-19(14) is 8.14×10^{-19} with the relative error of 14%.

Table 8 Organ doses calculated using MCNP code with phantom of 5 years due to semi-infinite source at twelve energies from 0.01 to 5 MeV (Gy per Bq s m^{-3})

Organ	5 MeV (10^{-13})	2MeV (10^{-14})	1MeV (10^{-14})	0.5MeV (10^{-14})	0.2 MeV (10^{-15})	0.1MeV (10^{-15})	0.07MeV (10^{-15})
Adrenals	2.69(2)	9.60(2)	4.65(2)	2.17(2)	8.07(2)	3.60(3)	2.60(9)
B surface	3.23(1)	13.1(1)	7.06(1)	4.45(1)	28.9(1)	21.3 (1)	16.6 (1)
Brain	2.97(1)	11.1(1)	5.23(1)	2.53(1)	9.71(2)	4.19(1)	2.54(1)
Breasts	2.70(5)	11.5 (3)	5.88(6)	2.60(4)	10.5(3)	5.01(5)	3.12(3)
Esophagus	2.76(2)	10.2(2)	4.75(2)	2.37(3)	8.15(3)	3.62(2)	2.27(3)
ST wall	2.81(1)	10.0(1)	4.66(1)	2.40(3)	8.63(2)	3.94(2)	2.47(2)
SI wall	2.72(1)	9.91(1)	4.61(1)	2.10(1)	8.06(1)	3.65(1)	2.14(1)
ULI wall	2.71(1)	10.4(2)	4.67(2)	2.24(1)	8.49(3)	3.71(2)	2.22(2)
LLI wall	2.76(2)	10.2(1)	4.66(2)	2.13(2)	8.25(2)	3.58(1)	2.15(2)
G. Bladder	2.77(3)	9.92(2)	4.39(3)	2.22(3)	8.41(3)	3.59(2)	2.16(3)
Heart	2.83(1)	10.2(2)	4.86(2)	2.29(1)	8.72(1)	3.94(2)	2.40(2)
Kidneys	2.81(1)	10.6(2)	4.94(2)	2.25(1)	8.79(2)	4.02(3)	2.52(3)
Liver	2.76(1)	10.4(1)	4.89(1)	2.37(2)	8.69(1)	4.04(1)	2.46(2)
Lung	2.96(1)	11.0(1)	5.27(1)	2.56(2)	9.74(1)	4.55(1)	2.90(2)
Muscle	2.96(1)	11.2(1)	5.49(1)	2.56(1)	9.72(1)	4.47(1)	2.85(1)
Ovaries	2.60(2)	9.51(2)	4.32(3)	2.32(6)	7.65(4)	3.61(3)	1.91(2)
Pancreas	2.70(1)	10.1(2)	4.33(2)	2.15(4)	8.43(4)	3.57(2)	2.09(2)
Bone R	2.96(1)	11.2(1)	5.22(1)	2.48(1)	9.35(1)	4.16(1)	2.51(1)
Skin	3.12(1)	12.1(1)	5.91(1)	2.88(1)	11.0(1)	5.17(1)	3.43(1)
Spleen	2.74(1)	10.2(1)	4.68(1)	2.38(3)	9.00(3)	4.04(2)	2.41(2)
Testes	2.95(4)	10.8(3)	5.04(3)	2.46(5)	10. 5(7)	4.23(4)	2.88(3)
Thymus	2.85(4)	10.4(1)	5.11(2)	2.42(3)	9.04(2)	4.28(2)	2.80(3)
Thyroid	2.75(3)	10.5(2)	5.36(4)	2.65(6)	8.91(3)	4.32(3)	2.89(6)
U bladder	2.70(1)	10.2(2)	4.77(2)	2.35(3)	8.46(2)	4.08(3)	2.35(4)
Uterus	2.58(2)	9.84(3)	4.43(2)	2.07(4)	7.44(4)	3.69(5)	1.99(3)
E	2.85	10.7	5.04	2.43	9.49	4.32	2.76

(*) The values in brackets are relative errors

Table 8 - continued

Organ	0.05MeV (10^{-15})	0.03MeV (10^{-16})	0.02MeV (10^{-17})	0.015MeV	0.01MeV
Adrenals	1.31(7)	2.31(8)	1.46 (6)	4.16e-19(17)	-
B surface	10.9(1)	29.6 (2)	47.6(1)	87.5e-18(1)	3.49e-18(1)
Brain	1.54(3)	2.68(2)	1.38(1)	2.72e-19(3)	-
Breasts	1.88(7)	11.1(2)	51.3(1)	2.62e-16(2)	5.45e-17(1)
Esophagus	1.07(3)	1.53(6)	0.44(7)	6.19e-20(20)	-
ST wall	1.55(5)	3.05(2)	3.46(3)	2.45e-18(3)	3.01e-21(40)
SI wall	1.15(2)	1.72(2)	0.69(2)	1.21e-19(5)	-
ULI wall	1.24(3)	2.17(3)	1.26(6)	2.73e-19(9)	-
LLI wall	1.11(4)	1.71(2)	0.74(5)	1.23e-19(30)	-
G. Bladder	1.13(4)	1.82(6)	0.66(6)	6.58e-20(25)	-
Heart	1.43(3)	2.57(2)	1.77(2)	9.19e-19(17)	5.75e-22(30)
Kidneys	1.45(3)	3.67(3)	6.08(5)	5.12e-18(3)	1.20e-20(40)
Liver	1.50(3)	3.08(2)	2.98(1)	1.94e-18(2)	9.49e-22(16)
Lung	1.74(2)	3.95(1)	3.95(1)	2.18e-18(2)	1.48e-21(11)
Muscle	1.84(1)	5.77(1)	15.9(1)	5.00e-17(1)	6.89e-18(1)
Ovaries	0.928(5)	1.04(6)	0.18(9)	-	-
Pancreas	1.11(4)	1.34(5)	2.68(6)	4.46e-21(40)	-
Bone R	1.35(1)	3.13(2)	4.99(1)	9.45e-18(1)	4.00e-19(1)
Skin	2.43(1)	11.3(1)	59.5(1)	3.67e-16(1)	1.75e-16(1)
Spleen	1.39(3)	2.79(2)	2.24(2)	7.70e-19(6)	-
Testes	1.72(5)	6.68(4)	24.2(3)	8.75e-17(4)	7.33e-18(6)
Thymus	1.66(5)	4.08(4)	5.51(3)	4.41e-18(4)	3.92e-21(40)
Thyroid	1.60(7)	4.89(3)	13.1(3)	3.84e-17(4)	2.18e-18(9)
U bladder	1.27(3)	3.01(3)	3.01(3)	1.91e-18(4)	1.98e-21(70)
Uterus	0.851(4)	1.27(5)	3.70(10)	1.17e-20(60)	-
E	1.61	4.52	11.3	3.93e-17	6.16e-18

(*) The values in brackets are relative errors
- The value of 4.16e-19(17) is 4.16×10^{-19} with the relative error of 17%.

Table 9 Organ doses calculated using MCNP code with phantom of 10 years due to semi-infinite source at twelve energies from 0.01 to 5 MeV (Gy per Bq s m^{-3})

Organ	5 MeV (10^{-13})	2MeV (10^{-14})	1MeV (10^{-14})	0.5MeV (10^{-14})	0.2 MeV (10^{-15})	0.1MeV (10^{-15})	0.07MeV (10^{-15})
Adrenals	2.69(4)	9.25(3)	4.20(4)	2.06(3)	7.41(3)	3.36(6)	1.90(4)
B surface	3.11(1)	12.6(3)	6.75(1)	4.26(1)	26.9 (1)	19.3(1)	14.6 (1)
Brain	2.93(1)	11.0 (1)	5.15(1)	2.43(1)	9.46(2)	4.13(2)	2.38(1)
Breasts	2.74(2)	11.3(4)	5.69(4)	2.60(4)	11.6(5)	4.72(4)	3.23(3)
Esophagus	2.66(1)	9.62(2)	4.53(2)	1.98(3)	7.87(5)	3.26(2)	1.76(1)
ST wall	2.63(1)	9.54(2)	4.59(2)	2.16(2)	8.29(3)	3.72(2)	2.22(2)
SI wall	2.61(2)	9.42(1)	4.30(1)	2.00(2)	7.51(1)	3.28(2)	1.85(1)
ULI wall	2.79(5)	9.46(1)	4.47(1)	1.98(2)	7.53(3)	3.46(2)	1.99(2)
LLI wall	2.71(3)	9.45(1)	4.34(2)	2.10(3)	7.58(2)	3.42(3)	1.88(2)
G. Bladder	2.50(2)	9.53(2)	3.99(2)	2.07(2)	7.42(3)	3.49(6)	1.93(3)
Heart	2.93(5)	9.85(1)	4.56(3)	2.21(2)	8.15(1)	3.81(3)	2.24(2)
Kidneys	2.70(2)	9.88(1)	4.71(3)	2.24(2)	8.39(3)	3.75(2)	2.31(2)
Liver	2.69(1)	9.86(1)	4.64(1)	2.16(2)	8.23(1)	3.76(1)	2.24(2)
Lung	2.99(3)	10. 9(1)	5.08(1)	2.42(1)	9.36(1)	4.24(2)	2.62(1)
Muscle	3.03(3)	11.2(1)	5.36(3)	2.47(1)	9.48(1)	4.33(1)	2.71(1)
Ovaries	2.57(4)	9.11(3)	4.10(3)	1.87(3)	7.00(3)	3.12(4)	1.80(5)
Pancreas	2.37(2)	8.62(1)	4.01(3)	1.96(3)	6.84(4)	3.10(3)	1.74(2)
Bone R	2.82(1)	10.5(3)	4.77(1)	2.25(2)	8.35(1)	3.63(1)	2.14(1)
Skin	2.46(3)	9.93(3)	4.49(1)	2.18(1)	8.45(1)	3.95(1)	2.60(1)
Spleen	2.68(1)	9.75(2)	4.59(2)	2.08(3)	8.18(2)	3.72(4)	2.23(2)
Testes	2.91(4)	10.5(4)	4.73(3)	2.28(3)	9.33(7)	4.66(1)	2.86(6)
Thymus	2.65(2)	10.6(4)	4.93(3)	2.31(3)	8.41(2)	3.89(2)	2.45(2)
Thyroid	2.70(2)	10.1(3)	5.30(6)	2.36(3)	8.65(3)	3.85(3)	2.67(3)
U bladder	2.71(2)	9.62(2)	4.59(2)	1.93(3)	7.95(5)	3.52(5)	2.15(2)
Uterus	2.76(7)	8.76(3)	4.05(3)	1.98(4)	7.14(4)	2.86(3)	1.80(4)
E	2.79	10.2	4.78	2.24	8.82	4.10	2.52

(*) The values in brackets are relative errors

Table 9 - continued

Organ	0.05MeV (10^{-16})	0.03MeV (10^{-16})	0.02MeV (10^{-18})	0.015MeV	0.01MeV
Adrenals	8.96(3)	1.53(4)	8.91(5)	8.63e-20(30)	-
B surface	93.7 (1)	22.6(1)	350(1)	5.97e-17(1)	2.09e-18(1)
Brain	12.6(1)	1.97(1)	8.97(1)	1.15e-19(8)	-
Breasts	21.0(5)	9.83(6)	448(1)	2.43e-16(2)	4.49e-17(4)
Esophagus	8.64(6)	0.890(2)	2.50(4)	2.13e-20(38)	-
ST wall	11.7(2)	2.21(1)	22.8(2)	1.53e-18(4)	1.22e-22(70)
SI wall	8.92(1)	1.13(1)	4.19(2)	4.92e-20(8)	-
ULI wall	9.58(1)	1.52(3)	8.45(5)	1.62e-19(20)	-
LLI wall	9.38(3)	1.21(3)	4.53(4)	3.11e-20(20)	-
G. Bladder	9.49(4)	1.18(2)	3.89(4)	2.39e-20(28)	-
Heart	11.4(2)	1.75(2)	11.4	5.12e-19(5)	2.24e-22(40)
Kidneys	12.3(2)	2.74(2)	37.7(1)	3.06e-18(4)	2.42e-21(50)
Liver	11.6(1)	2.19(1)	18.5(2)	8.84e-19(3)	1.38e-22(70)
Lung	13.9(1)	2.87(2)	25.4(1)	1.18e-18(3)	6.54e-22(35)
Muscle	24.7(1)	4.63(1)	176(1)	4.50e-17(1)	6.33e-18(1)
Ovaries	8.19(4)	0.689(2)	1.10(8)	-	-
Pancreas	8.99(6)	0.790(2)	1.25(5)	-	-
Bone R	11.0(1)	2.26(2)	36.4(1)	7.41e-18(1)	2.35e-19(1)
Skin	16.8(1)	7.62(1)	421(1)	2.99e-16(1)	1.42e-16(1)
Spleen	12.1(2)	2.00(3)	13.4(3)	3.92e-19(10)	-
Testes	15.6(3)	6.19(4)	223(3)	8.03e-17(3)	5.85e-18(6)
Thymus	13.4(2)	3.03(2)	35.7(2)	2.45e-18(5)	-
Thyroid	15.1(3)	4.30(2)	126(3)	3.47e-17(3)	1.58e-18(18)
U bladder	11.4(4)	2.09(5)	20.7(2)	1.14e-18(6)	-
Uterus	8.66(5)	0.904(5)	2.11(8)	-	-
E	13.7	4.03	95.4	3.51e-17	5.00e-18

(*) The values in brackets are relative errors
- The value of 8.63e-20(3) is 8.63×10^{-20} with the relative error of 30%.

Table 10 Organ doses calculated using MCNP code with phantom of 15 years due to semi-infinite source at twelve energies from 0.01 to 5 MeV (Gy per Bq s m^{-3})

Organ	5 MeV (10^{-13})	2MeV (10^{-14})	1MeV (10^{-14})	0.5MeV (10^{-14})	0.2 MeV (10^{-15})	0.1MeV (10^{-15})	0.07MeV (10^{-15})
Adrenals	2.60(4)	8.73(2)	3.88(3)	1.66(2)	6.73(3)	2.51(3)	1.65(6)
B surface	2.94(1)	11.52(1)	6.45(1)	3.98(2)	24.4(1)	17.0 (1)	12.8(1)
Brain	2.75(1)	10.72(1)	5.25(1)	2.36(2)	8.71(2)	3.99(2)	2.21(1)
Breasts	2.84(1)	10.74(1)	5.22(1)	2.58(2)	9.97(2)	4.66(2)	2.93(2)
Esophagus	2.47(1)	8.67(1)	3.95(2)	1.71(2)	6.51(2)	2.86(5)	1.43(5)
ST wall	2.55(3)	8.70(1)	4.22(1)	1.83(2)	7.22(1)	3.43(4)	1.87(2)
SI wall	2.48(1)	8.59(1)	4.05(2)	1.77(2)	6.40(1)	2.73(2)	1.61(3)
ULI wall	2.55(2)	8.67(1)	4.29(1)	1.73(3)	6.60(2)	2.96(3)	1.66(2)
LLI wall	2.64(5)	8.58(1)	4.03(1)	1.87(3)	7.19(5)	2.92(3)	1.51(2)
G. Bladder	2.40(2)	8.75(3)	4.18(2)	1.64(2)	6.40(2)	2.72(5)	1.50(2)
Heart	2.53(2)	9.20(2)	4.21(2)	1.90(3)	7.20(2)	3.16(3)	1.63(3)
Kidneys	2.57(2)	9.35(2)	4.37(2)	1.99(3)	7.35(1)	3.21(2)	1.93(3)
Liver	2.56(1)	9.20(1)	4.35(2)	1.92(3)	7.81(1)	3.22(2)	1.88(1)
Lung	2.74(1)	9.95(1)	4.67(1)	2.15(2)	8.93(1)	3.61(1)	2.30(3)
Muscle	2.82(1)	10.53(1)	5.01(1)	2.31(1)	8.78(1)	4.00(1)	2.44(1)
Ovaries	2.33(2)	8.41(4)	3.84(3)	1.81(5)	6.31(3)	2.63(6)	1.48(4)
Pancreas	2.43(3)	8.23(2)	3.82(2)	1.69(3)	6.26(4)	2.50(3)	1.52(5)
Bone R	2.65(1)	9.64(2)	4.55(2)	2.19(2)	7.94(2)	3.11(2)	1.84(2)
Skin	2.30(1)	9.01(1)	4.38(1)	2.08(1)	8.08(1)	3.85(1)	2.50(1)
Spleen	2.61(2)	9.32(3)	4.34(2)	1.89(3)	7.27(2)	3.01(3)	1.98(4)
Testes	2.68(3)	9.76(4)	4.45(2)	2.32(5)	8.94(4)	3.73(4)	2.41(5)
Thymus	2.53(2)	9.21(2)	4.19(2)	2.09(4)	8.26(5)	3.53(5)	2.16(4)
Thyroid	2.57(3)	10.26(3)	4.68(2)	2.34(4)	9.39(3)	3.91(6)	2.99(3)
U bladder	2.63(3)	9.40(3)	4.07(2)	1.87(2)	7.19(3)	2.97(3)	1.79(4)
Uterus	2.48(2)	8.34(2)	3.93(2)	1.67(2)	6.20(2)	2.59(4)	1.44(4)
E	2.65	9.58	4.45	2.14	8.23	3.55	2.20

(*) The values in brackets are relative errors

Table 10 - continued

Organ	0.05MeV (10^{-16})	0.03MeV (10^{-16})	0.02MeV	0.015MeV	0.01MeV
Adrenals	7.85(7)	1.24(6)	4.47e-18(6)	3.42e-20(20)	-
B surface	75.1(1)	17.4(1)	2.27e-16(0.2)	3.39e-17(0.3)	7.32e-19(1)
Brain	12.4(3)	1.84(1)	5.56e-18(2)	3.76e-20(6)	-
Breasts	19.6(2)	7.98(2)	2.35e-16(1)	6.83e-17(1)	6.14e-18(1)
Esophagus	5.98(3)	0.577(5)	9.87e-19(7)	1.66e-20(20)	-
ST wall	10.1(3)	1.62(3)	1.12e-17(2)	3.99e-19(4)	-
SI wall	7.23(3)	0.79(1)	1.89e-18(2)	1.65e-20(7)	-
ULI wall	7.83(4)	1.18(4)	3.92e-18(4)	3.42e-20(11)	-
LLI wall	7.62(5)	0.78(2)	1.95e-18(5)	9.35e-21(20)	-
G. Bladder	7.53(5)	0.85(2)	2.11e-18(7)	1.04e-20(35)	-
Heart	9.42(3)	1.17(3)	5.94e-18(2)	2.62e-19(3)	-
Kidneys	11.3(5)	2.29(4)	2.46e-17(2)	1.07e-18(3)	-
Liver	10.2(2)	1.74(2)	1.06e-17(2)	3.12e-19(2)	-
Lung	12.2(3)	2.02(1)	1.02e-17(3)	2.29e-19(3)	-
Muscle	15.6(1)	4.49(1)	11.2e-17(1)	3.24e-17(0.2)	3.53e-18(1)
Ovaries	6.22(8)	0.55(6)	1.65e-19(10)	-	-
Pancreas	5.99(4)	0.51(5)	3.54e-19(8)	-	-
Bone R	9.08(2)	1.75(2)	2.46e-17(2)	3.92e-18(2)	9.09e-20(5)
Skin	18.2(2)	8.45(1)	43. 6e-17(.1)	2.62e-16(0.2)	1.08e-16(0.1)
Spleen	10.4(4)	1.51(1)	6.90e-18(4)	1.15e-19(9)	-
Testes	16.5(7)	5.42(4)	1.55e-16(2)	3.59e-17(2)	1.10e-18(8)
Thymus	12.4(8)	2.49(2)	2.31e-17(3)	1.07e-18(6)	-
Thyroid	15.8(6)	4.92(2)	1.35e-16(2)	3.18e-17(2)	9.95e-19(20)
U bladder	9.87(6)	1.65(3)	1.22e-17(3)	4.03e-19(4)	-
Uterus	8.20(8)	0.61(3)	1.14e-18(13)	2.53e-21(30)	-
E	12.6	3.03	5.96e-17	1.58e-17	1.69e-18

(*) The values in brackets are relative errors
- The value of 3.42e-20(20) is 3.42×10^{-20} with the relative error of 20%.

Table 11 Organ doses calculated using MCNP code for adult phantom due to semi-infinite source at twelve energies from 0.01 to 5 MeV (Gy per Bq s m^{-3})

Organ	5MeV(10^{-13})	2 MeV(10^{-14})	1MeV(10^{-14})	0.5MeV(10^{-14})	0.2MeV(10^{-15})
Adrenals	2.43(5)	8.97(7)	4.07(3)	1.82(3)	6.46(3)
B surface	3.55(1)	13.0(1)	6.98(1)	4.06(1)	22.7(1)
Brain	2.95(1)	10.8(4)	5.19(2)	2.40(1)	8.53(2)
Breasts	3.22(4)	11.0(4)	5.34(2)	2.51(2)	9.87(3)
Esophagus	2.51(3)	9.39(4)	3.98(2)	1.83(2)	7.16(8)
ST wall	2.62(4)	8.79(2)	4.17(2)	2.00(3)	8.01(9)
SI wall	2.32(2)	8.63(3)	3.79(2)	1.88(3)	6.24(2)
ULI wall	2.30(2)	8.61(2)	4.22(6)	1.87(3)	6.80(4)
LLI wall	2.45(3)	9.00(3)	4.06(4)	1.93(3)	6.47(2)
G. Bladder	2.54(6)	9.06(6)	3.76(2)	1.96(2)	6.07(3)
Heart	2.55(3)	9.16(3)	4.33(3)	1.97(3)	6.96(2)
Kidneys	2.50(3)	9.32(3)	4.37(3)	1.96(2)	7.21(2)
Liver	2.78(6)	10.0(5)	4.20(2)	2.06(2)	7.36(2)
Lung	2.74(1)	10.3(3)	4.67(1)	2.25(2)	8.28(2)
Muscle	2.76(1)	10.3(2)	4.75(1)	2.26(1)	8.34(1)
Ovaries	2.45(9)	8.04(4)	3.63(4)	1.73(4)	6.73(6)
Pancreas	2.42(3)	8.59(3)	3.93(3)	1.80(2)	6.34(3)
Bone marrow	2.74(2)	9.97(2)	4.83(1)	2.18(1)	8.46(1)
Bone	2.85(2)	10.8(2)	5.15(1)	2.72(1)	12.8(1)
Skin	2.99(1)	11.5(1)	5.53(1)	2.73(1)	10.1(1)
Spleen	2.73(6)	9.14(2)	4.24(2)	2.05(2)	7.32(3)
Testes	2.66(9)	9.43(3)	4.51(2)	2.24(3)	8.52(5)
Thymus	2.61(5)	9.28(5)	4.22(2)	2.14(3)	7.78(5)
Thyroid	2.37(4)	10.0(3)	4.72(2)	2.29(5)	9.68(8)
U bladder	2.72(7)	9.22(6)	3.87(2)	1.87(2)	6.89(3)
Uterus	2.23(3)	8.53(4)	3.62(2)	1.89(2)	6.00(3)
E	2.64	9.46	4.44	2.10	8.19

(*) The values in brackets are relative errors

Table 11 - continued

Organ	0.1 MeV (10^{-15})	0.07 MeV (10^{-15})	0.05 MeV (10^{-16})	0.03 MeV (10^{-16})	0.02 MeV	0.015MeV	0.01 MeV
Adrenals	2.58(4)	1.51(4)	7.92(4)	1.09(4)	4.34e-18(9)	3.71e-20(40)	-
B surface	13.4(1)	10.3(1)	59.1(1)	13.5(1)	1.80e-16(1)	2.88e-17(2)	0.93e-18(4)
Brain	3.63(2)	2.18(2)	11.8(2)	1.33(2)	2.96e-18(2)	1.31e-20(15)	-
Breasts	4.32(2)	3.00(2)	19.9(2)	6.79(2)	2.09e-16(1)	6.10e-17(6)	4.49e-18(1)
Esophagus	2.62(3)	1.46(5)	6.45(4)	0.43(7)	8.12e-19(15)	6.04e-21(60)	-
ST wall	3.44(6)	1.96(8)	10.3(2)	1.49(4)	1.07e-17(6)	6.48e-18(9)	-
SI wall	2.68(3)	1.47(2)	7.23(4)	0.64(5)	1.84e-18(3)	1.58e-20(20)	-
ULI wall	2.81(3)	1.63(3)	7.85(3)	0.91(7)	3.97e-18(7)	4.29e-20(20)	-
LLI wall	2.64(3)	1.62(5)	7.58(3)	0.67(3)	1.69e-18(6)	1.31e-20(40)	-
G. Bladder	2.88(6)	1.58(8)	7.31(3)	0.81(9)	1.82e-18(7)	3.67e-20(40)	-
Heart	2.92(2)	1.67(2)	8.54(2)	1.10(4)	5.10e-18(2)	2.77e-19(15)	-
Kidneys	3.22(2)	1.96(3)	11.3(2)	2.08(2)	2.22e-17(5)	9.05e-19(5)	-
Liver	3.21(1)	1.95(2)	10.5(2)	1.42(2)	8.73e-18(1)	2.58e-19(3)	-
Lung	3.61(1)	2.27(1)	12.7(2)	1.88(2)	1.16e-17(3)	3.47e-19(3)	
Muscle	3.73(1)	2.35(1)	14.3(4)	3.55(1)	8.80e-17(1)	2.44e-17(1)	1.94e-18(1)
Ovaries	2.63(8)	1.32(4)	5.64(4)	0.38(7)	4.30e-19(15)	-	-
Pancreas	2.72(4)	1.41(3)	6.40(4)	0.44(5)	3.69e-19(11)	-	-
Bone marrow	3.47(1)	1.83(1)	9.15(1)	1.60(1)	2.51e-17(1)	4.95e-18(2)	1.54e-19(2)
Skin	4.73(1)	3.17(1)	22.0(1)	8.92(1)	4.69e-16(1)	2.81e-16(1)	1.05e-16(1)
Spleen	3.39(2)	1.84(2)	10.3(4)	1.34(2)	6.49e-18(8)	8.37e-20(20)	-
Testes	3.93(6)	2.43(4)	16.7(5)	5.31(3)	1.19e-16(2)	2.51e-17(2)	6.76e-19(4)
Thymus	3.57(7)	2.15(5)	12.8(7)	2.27(9)	2.02e-17(5)	1.05e-18(20)	-
Thyroid	4.09(4)	2.86(6)	16.0(4)	4.47(4)	1.12e-16(3)	2.39e-17(3)	3.70e-19(9)
U bladder	2.91(6)	1.94(3)	10.2(4)	1.39(3)	1.10e-17(3)	4.40e-19(11)	-
Uterus	2.72(6)	1.87(3)	6.24(3)	0.57(5)	8.79e-19(14)	3.31e-20(70)	-
E	3.55	2.19	12.4	2.77	5.41e-17	1.39e-17	1.47e-18

(*) The values in brackets are relative errors
- The value of 3.71e-20(40) is 3.71×10^{-20} with the relative error of 40%

Table 12 Effective doses calculated for respective phantoms (Sv per Bq s m^{-3})

Energy (MeV)	Newborn	1-year	5-years	10-years	15-years	Adult
0.01	1.45e-18	8.05e-18	6.16e-18	5.00e-18	1.69e-18	1.47e-18
0.015	5.64e-17	4.71e-17	3.93e-17	3.51e-17	1.58e-17	1.39e-17
0.02	1.58e-16	1.33e-16	1.13e-16	9.54e-17	5.96e-17	5.41e-17
0.03	6.01e-16	5.45e-16	4.52e-16	4.03e-16	3.03e-16	2.77e-16
0.05	1.90e-15	1.84e-15	1.61e-15	1.37e-15	1.26e-15	1.24e-15
0.07	3.08e-15	3.01e-15	2.76e-15	2.52e-15	2.20e-15	2.19e-15
0.1	4.77e-15	4.68e-15	4.32e-15	4.10e-15	3.55e-15	3.55e-15
0.2	1.03e-14	1.00e-14	9.49e-15	8.82e-15	8.23e-15	8.19e-15
0.5	2.64e-14	2.57e-14	2.43e-14	2.24e-14	2.14e-14	2.10e-14
1.0	5.38e-14	5.25e-14	5.04e-14	4.78e-14	4.45e-14	4.44e-14
2.0	1.15e-13	1.12e-14	1.07e-13	1.02e-13	9.58e-14	9.46e-14
5.0	3.03e-13	2.96e-13	2.85e-13	2.79e-13	2.65e-13	2.64e-13

Table 13 Conversion coefficients of effective dose (E/Air kerma) with difference aged phantoms (Sv Gy^{-1})

Energy (MeV)	Newborn	1-year	5-years	10-years	15-years	Adult
0.01	1.05e-2	5.85e-3	4.48e-3	3.63e-3	1.23e-3	1.07e-3
0.015	0.0327	0.0273	0.0228	0.0204	0.00914	0.00806
0.02	0.115	0.098	0.0824	0.0700	0.0436	0.0396
0.03	0.255	0.231	0.191	0.171	0.128	0.118
0.05	0.580	0.553	0.484	0.428	0.379	0.373
0.07	0.736	0.720	0.661	0.599	0.527	0.524
0.1	0.842	0.825	0.761	0.720	0.627	0.627
0.2	0.869	0.850	0.804	0.748	0.698	0.694
0.5	0.839	0.815	0.773	0.713	0.687	0.687
1.0	0.839	0.822	0.785	0.745	0.693	0.691
2.0	0.861	0.839	8.013	0.765	0.720	0.721
5.0	0.911	0.890	0.858	0.841	0.799	0.795

Table 14 Effective dose coefficients of radionuclides for air submersion (Sv per Bq s m^{-3})
(P0- New born phantom; P1- one year phantom; P5- five years phantom; P10- ten years phantom; P15- 15 years phantom; Padult- adult phantom; PadultE- adult phantom from FGR-12)

Nuclide	P0	P1	P5	P10	P15	Padult	PadultE
4-Be-7	2.65e-15	2.58e-15	2.44e-15	2.25e-15	2.15e-15	2.10e-15	2.22e-15
11-Na-22	1.18e-13	1.15e-13	1.10e-03	1.04e-13	9.72e-14	9.65e-14	1.01e-13
11-Na-24	2.39e-13	2.33e-13	2.22e-13	2.12e-13	2.00e-13	1.97e-13	2.08e-13
18-Ar-41	7.04e-14	6.87e-14	6.59e-14	6.27e-14	5.84e-14	5.82e-14	6.08e-14
19-K-40	8.69e-14	8.47e-14	8.12e-14	7.74e-14	7.22e-14	7.18e-14	7.51e-14
19-K-42	1.55e-14	1.51e-14	1.45e-14	1.38e-14	1.29e-14	1.28e-14	1.34e-14
21-Sc-46	1.08e-13	1.06e-13	1.01e-13	9.62e-14	8.96e-14	8.93e-14	9.32e-14
24-Cr-51	1.66e-15	1.61e-15	1.52e-15	1.40e-15	1.36e-15	1.31e-15	1.38e-15
25-Mn-54	4.46e-14	4.35e-14	4.16e-14	3.91e-14	3.67e-14	3.64e-14	3.82e-14
25-Mn-56	9.35e-14	9.12e-14	8.72e-14	8.29e-14	7.78e-14	7.70e-14	8.07e-14
26-Fe-59	6.45e-14	6.30e-14	6.06e-14	5.79e-14	5.38e-14	5.37e-14	5.56e-14
27-Co-56	1.99e-13	1.94e-13	1.85e-13	1.76e-13	1.66e-13	1.64e-13	1.72e-13
27-Co-57	5.89e-15	5.79e-15	5.33e-15	5.14e-15	4.79e-15	4.77e-15	4.94e-15
27-Co-58	5.19e-14	5.06e-14	4.83e-14	4.52e-14	4.26e-14	4.22e-14	4.42e-14
27-Co-60	1.37e-13	1.34e-13	1.28e-13	1.22e-13	1.14e-13	1.13e-13	1.18e-13
28-Ni-65	3.06e-14	2.87e-14	2.87e-14	2.75e-14	2.57e-14	2.55e-14	2.62e-14
30-Zn-65	3.13e-14	3.06e-14	2.94e-14	2.80e-14	2.60e-14	2.60e-14	2.70e-14
30-Zn-69m	2.21e-14	2.15e-14	2.04e-14	1.87e-14	1.79e-14	1.75e-14	1.85e-14
34-Se-75	1.95e-14	1.90e-14	1.79e-14	1.66e-14	1.55e-14	1.53e-14	1.63e-14
35-Br-83	3.75e-16	3.64e-16	3.46e-16	3.21e-16	3.05e-16	3.00e-16	3.15e-16
35-Br-84	1.01e-13	9.82e-14	9.81e-14	8.95e-14	8.44e-14	8.34e-14	8.77e-14
36-Kr-83m	8.65e-18	7.04e-18	5.65e-18	5.40e-18	2.64e-18	2.15e-18	2.20e-18
36-Kr-85m	7.89e-15	7.74e-15	7.18e-15	6.87e-15	6.20e-15	6.16e-15	6.64e-15
36-Kr-85	1.17e-16	1.14e-16	1.08e-16	9.96e-17	9.51e-17	9.32e-17	9.82e-17
36-Kr-87	4.45e-14	4.33e-14	4.13e-14	3.90e-14	3.70e-14	3.64e-14	3.83e-14
36-Kr-88	1.12e-13	1.09e-13	1.04e-13	9.90e-14	9.32e-14	9.21e-14	9.68e-14
37-Rb-86	5.04e-15	4.91e-15	4.71e-15	4.48e-15	4.17e-15	4.16e-15	4.34e-15
37-Rb-88	6.39e-14	6.22e-14	5.94e-14	5.67e-14	5.35e-14	5.28e-14	5.55e-14
37-Rb-89	1.15e-13	1.13e-13	1.08e-13	1.03e-13	9.60e-14	9.53e-14	9.98e-14

Table 14 - continued

Nuclide	P0	P1	P5	P10	P15	Padult	PadultE
38-Sr-89	4.65e-18	4.54e-18	4.35e-18	4.10e-18	3.84e-18	3.82e-18	3.99e-18
38-Sr-91	3.78e-14	3.69e-14	3.53e-14	3.34e-14	3.12e-14	3.10e-14	3.24e-14
38-Sr-92	7.32e14	7.16e-14	6.88e-14	6.60e-14	6.16e-14	6.12e-14	6.30e-14
38-Sr-93	1.25e-13	1.22e-13	1.16e-13	1.10e-13	1.03e-13	1.02e-13	1.07e-13
39-Y-90m	3.32e-14	3.23e-14	3.06e-14	2.82e-14	2.68e-14	2.64e-14	2.78e-14
39-Y-91m	2.79e-14	2.71e-14	2.58e-14	2.38e-14	2.27e-14	2.23e-14	2.35e-14
39-Y-91	1.97e-16	1.92e-16	1.85e-16	1.76e-16	1.64e-16	1.63e-16	1.70e-16
39-Y-92	1.36e-14	1.33e-14	1.27e-14	1.20e-14	1.12e-14	1.12e-14	1.17e-14
39-Y-93	5.27e-15	5.13e-15	4.90e-15	4.63e-15	4.35e-15	4.31e-15	4.52e-15
40-Zr-95	3.88e-14	3.79e-14	3.63e-14	3.41e-14	3.19e-14	3.17e-14	3.32e-14
40-Zr-97	4.68e-14	4.57e-14	4.37e-14	4.11e-14	3.85e-14	3.83e-14	4.00e-14
41-Nb-93m	1.45e-17	1.20e-17	1.01e-17	8.62e-18	4.92e-18	4.47e-18	4.89e-18
41-Nb-95m	3.32e-15	3.24e-15	3.05e-15	2.82e-15	2.65e-15	2.62e-15	2.75e-15
41-Nb-95	4.08e-14	3.97e-14	3.79e-14	3.55e-14	3.34e-14	3.31e-14	3.47e-14
41-Nb-97m	3.86e-14	3.77e-14	3.60e-14	3.39e-14	3.17e-14	3.16e-14	3.30e-14
41-Nb-97	3.53e-14	3.44e-14	3.29e-14	3.08e-14	2.89e-14	2.87e-14	3.00e-14
42-Mo-93	5.45e-17	4.40e-17	3.75e-17	3.17e-17	1.67e-17	1.52e-17	1.64e-17
42-Mo-99	7.81e-15	7.62e-15	7.24e-15	6.79e-15	6.37e-15	6.30e-15	6.64e-15
42-Mo-101	8.40e-14	8.19e-14	7.83e-14	7.41e-14	6.94e-14	6.88e-14	7.21e-14
43-Tc-99m	6.27e-15	6.16e-15	5.66e-15	5.51e-15	4.83e-15	4.83e-15	5.29e-15
43-Tc-101	1.77e-14	1.72e-14	1.63e-14	1.50e-14	1.42e-14	1.40e-14	1.47e-14
44-Ru-103	2.62e-14	2.54e-14	2.42e-14	2.23e-14	2.12e-14	2.08e-14	2.20e-14
44-Ru-105	3.93e-14	3.82e-14	3.64e-14	3.39e-14	3.21e-14	3.16e-14	3.33e-14
45-Rh-103m	1.45e-17	1.25e-17	1.05e-17	8.97e-18	5.86e-18	5.33e-18	5.92e-18
45-Rh-105	4.03e-15	3.92e-15	3.70e-15	3.39e-15	3.24e-15	3.17e-15	3.35e-15
45-Rh-106	1.09e-14	1.07e-14	1.02e-14	9.42e-15	8.94e-15	8.81e-15	9.26e-15
47-Ag-110m	1.46e-13	1.43e-13	1.37e-13	1.29e-13	1.21e-13	1.20e-13	1.25e-13
47-Ag-111	1.38e-15	1.34e-15	1.27e-15	1.16e-15	1.11e-15	1.09e-15	1.15e-15
50-Sn-117m	7.26e-15	7.13e-15	6.55e-15	6.34e-15	5.60e-15	5.59e-15	6.05e-15
50-Sn-126	2.60e-15	2.53e-15	2.42e-15	2.27e-15	2.13e-15	2.11e-15	2.21e-15

Table 14 - continued

Nuclide	P0	P1	P5	P10	P15	Padult	PadultE
51-Sb-124	1.01e-13	9.99e-14	9.46e-14	8.97e-14	8.40e-14	8.34e-14	8.62e-14
51-Sb-125	2.24e-14	2.18e-14	2.06e-14	1.91e-14	1.81e-14	1.78e-14	1.87e-14
51-Sb-126m	8.21e-14	7.99e-14	7.60e-14	7.06e-14	6.70e-14	6.60e-14	6.94e-14
51-Sb-126	1.47e-13	1.43e-13	1.36e-13	1.27e-13	1.20e-13	1.19e-13	1.24e-13
51-Sb-127	3.67e-14	3.57e-14	3.40e-14	3.16e-14	2.99e-14	2.95e-14	3.10e-14
51-Sb-128	1.73e-13	1.68e-13	1.61e-13	1.50e-14	1.42e-13	1.40e-13	1.47e-13
51-Sb-129	7.49e-14	7.30e-14	6.99e-14	6.62e-14	6.19e-14	6.15e-14	6.38e-14
51-Sb-130	1.75e-13	1.70e-13	1.62e-13	1.53e-13	1.45e-13	1.42e-13	1.49e-13
51-Sb-131	1.13e-13	1.10e-13	1.06e-13	1.00e-13	9.38e-14	9.32e-14	9.75e-14
52-Te-123m	6.95e-15	6.81e-15	6.26e-15	6.06e-15	5.36e-15	5.34e-15	5.78e-15
52-Te-125m	6.52e-16	5.90e-16	4.90e-16	4.25e-16	3.26e-16	2.99e-16	3.30e-16
52-Te-127m	2.35e-16	2.16e-16	1.84e-16	1.66e-16	1.30e-16	1.21e-16	1.33e-16
52-Te-127	2.55e-16	2.48e-16	2.34e-06	2.15e-16	2.06e-16	2.01e-16	2.12e-16
52-Te-129m	1.71e-15	1.65e-15	1.56e-15	1.45e-15	1.35e-15	1.34e-15	1.42e-15
52-Te-129	3.20e-15	3.04e-15	2.89e-15	2.67e-15	2.54e-15	2.50e-15	2.63e-15
52-Te-131m	7.84e-14	7.65e-14	7.31e-14	6.88e-14	6.45e-14	6.40e-14	6.68e-14
52-Te-131	2.20e-14	2.15e-14	2.03e-14	1.92e-14	1.78e-14	1.76e-14	1.86e-14
52-Te-132	1.12e-14	1.10e-14	1.03e-14	9.54e-15	8.86e-15	8.74e-15	9.21e-15
52-Te-133m	9.88e-14	9.63e-14	9.22e-14	8.71e-14	8.14e-14	8.09e-14	8.64e-14
52-Te-133	6.56e-14	6.39e-14	6.10e-14	5.75e-14	5.40e-14	5.35e-14	4.11e-14
52-Te-134	4.56e-14	4.44e-14	4.21e-14	3.92e-14	3.70e-14	3.65e-14	3.84e-14
53-I-129	5.30e-16	4.51e-16	4.03e-16	3.61e-16	2.76e-16	2.55e-16	2.79e-16
53-I-130	1.17e-13	1.14e-13	1.09e-13	1.01e-13	9.58e-14	9.45e-14	9.93e-14
53-I-131	2.01e-14	1.96e-14	1.85e-14	1.70e-14	1.63e-14	1.59e-14	1.68e-14
53-I-132	1.12e-13	1.09e-13	1.04e-13	9.71e-14	9.16e-14	9.09e-14	9.51e-14
53-I-133	3.25e-14	3.16e-14	3.01e-14	2.79e-14	2.65e-14	2.61e-14	2.74e-14
53-I-134	1.43e-13	1.39e-13	1.33e-13	1.25e-13	1.18e-13	1.17e-13	1.22e-13
53-I-135	8.87e-14	8.65e-14	8.28e-14	7.87e-14	7.36e-14	7.31e-14	7.65e-14
54-Xe-123	3.35e-14	3.26e-14	3.09e-14	2.91e-14	2.72e-14	2.68e-14	2.83e-14
54-Xe-125	1.30e-14	1.27e-14	1.19e-14	1.11e-14	1.03e-14	1.02e-14	1.07e-14
54-Xe-127	1.16e-14	1.08e-14	1.06e-14	9.78e-15	9.14e-15	9.02e-15	9.50e-15
54-Xe-131m	5.10e-16	4.76e-16	4.09e-16	3.77e-16	3.04e-16	2.89e-16	3.15e-16
54-Xe-133m	1.56e-15	1.50e-15	1.38e-15	1.26e-15	1.15e-15	1.12e-15	1.19e-15
54-Xe-133	1.78e-15	1.71e-15	1.55e-15	1.42e-15	1.22e-15	1.20e-15	1.32e-15
54-Xe-135m	2.25e-14	2.19e-14	2.08e-14	1.92e-14	1.82e-14	1.79e-14	1.89e-14
54-Xe-135	1.28e-14	1.25e-14	1.18e-14	1.09e-14	1.03e-14	1.02e-14	1.07e-14
54-Xe-138	6.18e-14	6.02e-14	5.74e-14	5.44e-14	5.12e-14	5.06e-14	5.32e-14
55-Cs-134m	1.01e-15	9.78e-16	8.80e-16	8.41e-16	7.18e-16	7.08e-16	7.79e-16
55-Cs-134	8.23e-14	8.06e-14	7.69e-14	7.18e-14	6.78e-14	6.70e-14	7.03e-14
55-Cs-136	1.14e-13	1.11e-13	1.06e-13	1.01e-13	9.38e-14	9.33e-14	9.75e-14
55-Cs-138	1.32e-13	1.28e-13	1.23e-13	1.16e-13	1.09e-13	1.08e-13	1.14e-13

Table 14 - continued

Nuclide	P0	P1	P5	P10	P15	Padult	PadultE
56-Ba-137m	3.16e-14	3.08e-14	2.93e-14	2.73e-14	2.58e-14	2.55e-14	2.68e-14
56-Ba-139	2.25e-15	2.21e-15	2.05e-15	1.98e-15	1.77e-15	1.77e-15	1.90e-15
56-Ba-140	9.40e-15	9.14e-15	8.66e-15	7.99e-15	7.59e-15	7.45e-15	7.85e-15
57-La-140	1.28e-13	1.25e-13	1.19e-13	1.13e-13	1.06e-13	1.05e-13	1.10e-13
57-La-141	1.48e-15	1.44e-15	1.38e-15	1.32e-15	1.23e-15	1.22e-15	1.28e-15
57-La-142	1.36e-13	1.32e-13	1.26e-13	1.20e-13	1.14e-13	1.12e-13	1.18e-13
58-Ce-141	3.66e-15	3.59e-15	3.28e-15	3.19e-15	2.79e-15	2.79e-15	3.04e-15
58-Ce-143	1.40e-14	1.36e-14	1.27e-14	1.17e-14	1.12e-14	1.10e-14	1.14e-14
59-Pr-145	1.02e-15	9.92e-16	9.48e-16	8.93e-16	8.35e-16	8.29e-16	8.67e-14
60-Nd-147	6.82e-15	6.62e-15	6.20e-15	5.73e-15	5.32e-15	5.23e-15	5.56e-15
61-Pm-148m	1.05e-13	1.03e-13	9.76e-14	9.08e-14	8.61e-14	8.49e-14	8.92e-14
61-Pm-148	3.16e-14	3.08e-14	2.95e-14	2.79e-14	2.61e-14	2.59e-14	2.71e-14
61-Pm-149	6.20e-16	6.04e-16	5.72e-16	5.28e-16	5.01e-16	4.92e-16	5.18e-16
61-Pm-151	1.69e-14	1.65e-14	1.56e-14	1.45e-14	1.37e-14	1.35e-14	1.42e-14
63-Eu-52m	1.62e-14	1.58e-14	1.49e-14	1.42e-14	1.32e-14	1.31e-14	1.38e-14
63-Eu-152	6.24e-14	6.09e-14	5.82e-14	5.51e-14	5.12e-14	5.10e-14	5.31e-14
63-Eu-154	6.05e-14	5.90e-14	5.65e-14	5.36e-14	4.98e-14	4.96e-14	5.17e-14
63-Eu-155	2.73e-15	2.67e-15	2.44e-15	2.28e-15	1.98e-15	1.97e-15	2.16e-15
63-Eu-156	6.83e-14	6.65e-14	6.37e-14	6.05e-14	5.66e-14	5.62e-14	5.89e-14
72-Hf-181	2.76e-14	2.68e-14	2.53e-14	2.34e-14	2.21e-14	2.17e-14	2.30e-14
73-Ta-182	6.93e-14	6.77e-14	6.49e-14	6.18e-14	5.75e-14	5.72e-14	5.95e-14
74-W-187	2.35e-14	2.29e-14	2.17e-14	2.02e-14	1.90e-14	1.88e-14	1.98e-14
81-Tl-208	1.89e-13	1.87e-13	1.79e-13	1.70e-13	1.61e-14	1.58e-13	1.67e-13
82-Pb-210	8.27e-17	7.80e-17	6.60e-17	6.04e-17	4.90e-17	4.68e-17	4.86e-17
82-Pb-212	7.21e-15	7.03e-15	6.61e-15	6.10e-15	5.69e-15	5.61e-15	5.95e-15
82-Pb-214	1.30e-14	1.27e-14	1.20e-14	1.10e-14	1.04e-14	1.02e-14	1.08e-14
83-Bi-212	5.56e-15	5.42e-15	5.18e-15	4.89e-15	4.64e-15	4.61e-15	4.71e-15
83-Bi-214	8.27e-14	8.06e-14	7.70e-14	7.32e-14	6.86e-14	6.80e-14	7.12e-14
88-Ra-224	5.28e-16	5.17e-16	4.88e-16	4.50e-16	4.25e-16	4.19e-16	4.41e-16
88-Ra-226	3.67e-16	3.60e-16	3.36e-16	3.18e-16	2.90e-16	2.89e-16	3.08e-16
89-Ac-228	4.64e-14	4.52e-14	4.33e-14	4.09e-14	3.82e-14	3.80e-14	3.96e-14

Table 14 - continued

Nuclide	P0	P1	P5	P10	P15	Padult	PadultE
90-Th-228	1.05e-16	1.02e-16	9.38e-17	8.76e-17	7.70e-17	7.64e-17	8.28e-17
90-Th-231	6.02e-16	5.78e-16	5.24e-16	4.84e-16	4.09e-16	4.08e-16	4.45e-16
90-Th-232	1.36e-17	1.24e-17	1.10e-17	1.01e-17	7.71e-18	7.47e-18	8.01e-18
90-Th-234	4.10e-16	4.00e-16	3.67e-16	3.40e-16	2.95e-16	2.94e-16	3.22e-16
91-Pa-233	1.10e-14	1.07e-14	1.00e-14	9.26e-15	8.69e-15	8.54e-15	9.08e-15
92-U-232	2.30e-17	2.06e-17	1.82e-17	1.55e-17	1.20e-17	1.15e-17	1.25e-17
92-U-234	1.41e-17	1.26e-17	1.09e-17	9.89e-18	6.93e-18	6.63e-18	7.12e-18
92-U-235	8.07e-15	7.90e-15	7.38e-15	7.01e-15	6.37e-15	6.35e-15	6.78e-15
92-U-236	9.66e-18	8.23e-18	7.00e-18	6.31e-18	3.95e-18	3.69e-18	3.91e-18
92-U-237	6.37e-15	6.22e-15	5.78e-15	5.37e-15	4.90e-15	4.81e-15	5.18e-15
92-U-238	7.42e-18	6.28e-18	5.31e-18	4.78e-18	2.92e-18	2.70e-18	2.87e-18
93-Np-237	1.11e-15	1.06e-15	9.77e-16	9.11e-16	7.83e-16	7.76e-16	8.53e-16
93-Np-238	3.46e-14	3.37e-14	3.23e-14	3.07e-14	2.86e-14	2.85e-14	2.97e-14
93-Np-239	8.98e-15	8.80e-15	8.20e-15	7.66e-15	6.99e-15	6.91e-15	7.43e-15
94-Pu-236	1.21e-17	1.01e-18	8.56e-18	7.53e-18	4.47e-18	4.11e-18	4.42e-18
94-Pu-238	1.04e-17	8.60e-18	6.97e-18	6.37e-08	3.60e-18	3.27e-18	3.53e-18
94-Pu-239	6.76e-18	5.94e-18	5.20e-18	4.65e-18	3.32e-18	3.16e-18	3.38e-18
94-Pu-240	9.94e-18	8.25e-18	6.95e-18	6.10e-18	3.50e-18	3.20e-18	3.44e-18
94-Pu-242	8.33e-18	6.92e-18	5.84e-18	5.13e-18	2.96e-18	2.71e-18	2.96e-18
95-Am-241	9.45e-16	9.13e-16	8.23e-16	7.34e-16	6.38e-16	6.31e-16	6.70e-16
95-Am-242m	3.96e-17	3.44e-17	2.95e-17	2.60e-17	1.76e-17	1.65e-17	1.80e-17
95-Am-242	6.56e-16	6.38e-16	5.86e-16	5.56e-16	4.78e-16	4.77e-16	5.25e-16
95-Am-243	2.45e-15	2.38e-15	2.19e-15	2.00e-15	1.75e-15	1.74e-15	1.90e-15
96-Cm-242	1.11e-17	1.02e-17	8.66e-18	6.71e-18	3.88e-18	3.52e-18	3.82e-18
96-Cm-243	5.94e-15	5.80e-15	5.42e-15	5.06e-15	4.62e-15	4.57e-15	4.91e-15
96-Cm-244	9.43e-18	7.82e-18	6.58e-18	5.70e-18	3.28e-18	2.96e-18	3.23e-18
96-Cm-245	4.74e-15	4.64e-15	4.28e-15	4.08e-15	3.57e-15	3.57e-15	3.92e-15
96-Cm-247	1.65e-14	1.60e-14	1.52e-14	1.39e-14	1.33e-14	1.30e-14	1.37e-14
96-Cm-248	6.88e-18	5.71e-18	4.81e-18	4.16e-18	2.39e-18	2.17e-18	2.36e-18

This is a blank page.

国際単位系（SI）と換算表

表1　SI基本単位および補助単位

量	名称	記号
長さ	メートル	m
質量	キログラム	kg
時間	秒	s
電流	アンペア	A
熱力学温度	ケルビン	K
物質量	モル	mol
光度	カンデラ	cd
平面角	ラジアン	rad
立体角	ステラジアン	sr

表2　SIと併用される単位

名称	記号
分，時，日	min，h，d
度，分，秒	°，′，″
リットル	l，L
トン	t
電子ボルト	eV
原子質量単位	u

1 eV=1.60218×10^{-19}J

1 u=1.66054×10^{-27}kg

表5　SI接頭語

倍数	接頭語	記号
10^{18}	エクサ	E
10^{15}	ペタ	P
10^{12}	テラ	T
10^{9}	ギガ	G
10^{6}	メガ	M
10^{3}	キロ	k
10^{2}	ヘクト	h
10^{1}	デカ	da
10^{-1}	デシ	d
10^{-2}	センチ	c
10^{-3}	ミリ	m
10^{-6}	マイクロ	μ
10^{-9}	ナノ	n
10^{-12}	ピコ	p
10^{-15}	フェムト	f
10^{-18}	アト	a

表3　固有の名称をもつSI組立単位

量	名称	記号	他のSI単位による表現
周波数	ヘルツ	Hz	s^{-1}
力	ニュートン	N	$m\cdot kg/s^2$
圧力，応力	パスカル	Pa	N/m^2
エネルギー,仕事,熱量	ジュール	J	N·m
工率，放射束	ワット	W	J/s
電気量，電荷	クーロン	C	A·s
電位，電圧，起電力	ボルト	V	W/A
静電容量	ファラド	F	C/V
電気抵抗	オーム	Ω	V/A
コンダクタンス	ジーメンス	S	A/V
磁束	ウェーバ	Wb	V·s
磁束密度	テスラ	T	Wb/m^2
インダクタンス	ヘンリー	H	Wb/A
セルシウス温度	セルシウス度	℃	
光束	ルーメン	lm	cd·sr
照度	ルクス	lx	lm/m^2
放射能	ベクレル	Bq	s^{-1}
吸収線量	グレイ	Gy	J/kg
線量等量	シーベルト	Sv	J/kg

表4　SIと共に暫定的に維持される単位

名称	記号
オングストローム	Å
バーン	b
バール	bar
ガル	Gal
キュリー	Ci
レントゲン	R
ラド	rad
レム	rem

1 Å=0.1nm=10^{-10}m

1 b=100fm^2=10^{-28}m^2

1 bar=0.1MPa=10^5Pa

1 Gal=1cm/s^2=10^{-2}m/s^2

1 Ci=3.7×10^{10}Bq

1 R=2.58×10^{-4}C/kg

1 rad=1cGy=10^{-2}Gy

1 rem=1cSv=10^{-2}Sv

(注)

1．表1－5は「国際単位系」第5版，国際度量衡局1985年刊行による。ただし，1 eVおよび1 uの値はCODATAの1986年推奨値によった。

2．表4には海里，ノット，アール，ヘクタールも含まれているが日常の単位なのでここでは省略した。

3．barは，JISでは流体の圧力を表わす場合に限り表2のカテゴリーに分類されている。

4．EC閣僚理事会指令ではbar，barnおよび「血圧の単位」mmHgを表2のカテゴリーに入れている。

換算表

力	N(=10^5dyn)	kgf	lbf
	1	0.101972	0.224809
	9.80665	1	2.20462
	4.44822	0.453592	1

粘度　1 Pa·s(N·s/m^2)=10 P(ポアズ)(g/(cm·s))

動粘度　1m^2/s=10^4St(ストークス)(cm^2/s)

圧力	MPa(=10bar)	kgf/cm^2	atm	mmHg(Torr)	lbf/in^2(psi)
	1	10.1972	9.86923	7.50062×10^3	145.038
	0.0980665	1	0.967841	735.559	14.2233
	0.101325	1.03323	1	760	14.6959
	1.33322×10^{-4}	1.35951×10^{-3}	1.31579×10^{-3}	1	1.93368×10^{-2}
	6.89476×10^{-3}	7.03070×10^{-2}	6.80460×10^{-2}	51.7149	1

エネルギー・仕事・熱量	J(=10^7 erg)	kgf·m	kW·h	cal(計量法)	Btu	ft·lbf	eV
	1	0.101972	2.77778×10^{-7}	0.238889	9.47813×10^{-4}	0.737562	6.24150×10^{18}
	9.80665	1	2.72407×10^{-6}	2.34270	9.29487×10^{-3}	7.23301	6.12082×10^{19}
	3.6×10^6	3.67098×10^5	1	8.59999×10^5	3412.13	2.65522×10^6	2.24694×10^{25}
	4.18605	0.426858	1.16279×10^{-6}	1	3.96759×10^{-3}	3.08747	2.61272×10^{19}
	1055.06	107.586	2.93072×10^{-4}	252.042	1	778.172	6.58515×10^{21}
	1.35582	0.138255	3.76616×10^{-7}	0.323890	1.28506×10^{-3}	1	8.46233×10^{18}
	1.60218×10^{-19}	1.63377×10^{-20}	4.45050×10^{-26}	3.82743×10^{-20}	1.51857×10^{-22}	1.18171×10^{-19}	1

1 cal= 4.18605J（計量法）

= 4.184J（熱化学）

= 4.1855J（15℃）

= 4.1868J（国際蒸気表）

仕事率　1 PS(仏馬力)

= 75 kgf·m/s

= 735.499W

放射能	Bq	Ci
	1	2.70270×10^{-11}
	3.7×10^{10}	1

吸収線量	Gy	rad
	1	100
	0.01	1

照射線量	C/kg	R
	1	3876
	2.58×10^{-4}	1

線量当量	Sv	rem
	1	100
	0.01	1

(86年12月26日現在)

Calculation of Age-dependent Dose Conversion Coefficients for Radionuclides Uniformly Distributed in Air